Binding of Serum Response Factor to Cystic Fibrosis Transmembrane Conductance regulator CArG-like elements, as a new potential CFTR transcriptional regulator pathway

Céline René, Florence Iral, Magali Taulan, Julien Doudement, Aurore L'Honoré, Catherine Gerbon, Jacques Demaille, Mireille Claustres, Marie-Catherine Romey

Published online September 16, 2005

Nucleic Acids Research, 2005, Vol. 33, No. 16 ***5271–5290***
doi:10.1093/nar/gki837

Binding of serum response factor to cystic fibrosis transmembrane conductance regulator CArG-like elements, as a new potential CFTR transcriptional regulation pathway

Céline René, Magali Taulan, Florence Iral, Julien Doudement, Aurore L'Honoré[1,2], Catherine Gerbon, Jacques Demaille[3], Mireille Claustres and Marie-Catherine Romey*

Laboratoire de Génétique Moléculaire et Chromosomique, Institut Universitaire de Recherche Clinique, Montpellier, France, [1]Laboratoire de Prolifération et Différentiation Cellulaire, Institut de Génétique Humaine, Montpellier, France, [2]Laboratoire de Génétique Moléculaire, Institut de Recherches Cliniques de Montréal, Quebec, Canada and [3]Centre de Séquençage Génomique, Institut de Génétique Humaine, Montpellier, France

Revised as resubmission August 25, 2005; Accepted August 30, 2005

ABSTRACT

***CFTR* expression is tightly controlled by a complex network of ubiquitous and tissue-specific *cis*-elements and *trans*-factors. To better understand mechanisms that regulate transcription of *CFTR*, we examined transcription factors that specifically bind a *CFTR* CArG-like motif we have previously shown to modulate *CFTR* expression. Gel mobility shift assays and chromatin immunoprecipitation analyses demonstrated the *CFTR* CArG-like motif binds serum response factor both *in vitro* and *in vivo*. Transient co-transfections with various SRF expression vector, including dominant-negative forms and small interfering RNA, demonstrated that SRF significantly increases *CFTR* transcriptional activity in bronchial epithelial cells. Mutagenesis studies suggested that in addition to SRF other co-factors, such as Yin Yang 1 (YY1) previously shown to bind the *CFTR* promoter, are potentially involved in the *CFTR* regulation. Here, we show that functional interplay between SRF and YY1 might provide interesting perspectives to further characterize the underlying molecular mechanism of the basal *CFTR* transcriptional activity. Furthermore, the identification of multiple CArG binding sites in highly conserved *CFTR* untranslated regions, which form specific SRF complexes, provides direct evidence for a considerable role of SRF in the *CFTR* transcriptional regulation into specialized epithelial lung cells.**

INTRODUCTION

Expression of the cystic fibrosis transmembrane conductance regulator (*CFTR*) gene occurs in a subset of specialized cells of epithelial origin (1–3) and is tightly regulated both temporally and spatially (4,5). However, no clear mechanism responsible for this regulation has yet been reported in part due to the complexity of the non-coding regions structure of the *CFTR* gene.

Despite the absence of a TATA element, the transcription of the *CFTR* gene may be initiated through several discrete start sites (6,7), including those that are tissue-specific (8). An intact CCAAT consensus is also required for accurate transcript initiation (9). Both basal and cAMP-mediated regulation of *CFTR* transcription involve a weak cAMP response element (CRE) nucleotide consensus (10,11) in tandem with a consensus inverted CCAAT element or Y box (9). In addition, *CFTR* transcription may be modulated by additional overlapping *cis*-acting elements, including a polymorphic YY1 site, located in the human minimal *CFTR* promoter (12). *CFTR* promoter activity may be enhanced by exogenous transfected NF-κB via its binding to the –1103 κB element (13). *CFTR* expression is also regulated through interactions with factors involved in remodeling of chromatin structure, such as CDP/*cut* and hGCN5 (14).

Because none of these *cis*-acting elements confers tissue-specific control of *CFTR* expression, several studies focused on identifying potential regulatory elements that lie mainly outside the coding region. Extensive analyses of the chromatin structure identified multiple clusters of DNase I-hypersensitive sites (DHSs) (15,16), some of which contain tissue-specific enhancer elements (17,18). Multiple binding sites for a tissue-specific transcription factor, called

*To whom correspondence should be addressed. Tel: +33 4 67 41 53 60; Fax: +33 4 67 41 53 65; Email: Marie-Catherine.Romey@igh.cnrs.fr
The authors wish it to be known that, in their opinion, the first three authors should be regarded as joint First Authors

HNF1α, recently identified in various DHS core, modulate likewise *CFTR* expression (19). Despite extensive studies, the transcriptional regulatory networks of *CFTR* expression remain to be unraveled.

Our current model for the regulation of human *CFTR* expression proposes that multiple transcription factors interact with previously reported polymorphic and composite *cis*-acting elements encompassing a CArG-like motif (12,20). The CArG box ($CC(A/T)_6GG$), originally defined as the core component of the serum response element (SRE), is found in the 5′ region of immediate early response genes, such as *c-fos* (21), and in many muscle-specific gene promoters (22). This DNA element binds serum response factor (SRF), highly regulated and interactive transcription factor, which is phylogenetically conserved and belongs to the MADS box family of proteins, with MCM1, Agamous, Deficiens and SRF (23). Although SRF is particularly enriched in skeletal, cardiac and smooth muscle lineages (24,25), it is also expressed in a variety of human cell lines from distinct tissue origins (26), and, to a lesser extent, in ectoderm-derived tissue such as gastric epithelium (27). Interestingly, it has been shown that *Drosophila* SRF homolog is expressed in a subset of tracheal cells and regulates cytoplasmic outgrowth during terminal branching of the tracheal system (28). Hence, it has been suggested that SRF plays an essential role in the formation of the respiratory system. Moreover, it has been recently shown that SRF is involved in myofibroblast differentiation during lung damage (29). Therefore, we hypothesized that *trans*-acting factors interacting with CArG-like motif, such as SRF, could be important in *CFTR* expression regulation. We provided evidence that SRF is expressed in bronchial epithelial cell expressing endogenous CFTR protein. Through the use of combined gel mobility shift–chromatin immunoprecipitation (ChIP) assays, we first demonstrated that SRF protein binds, both *in vitro* and *in vivo*, the *CFTR* minimal promoter region spanning the CArG-like motif. Mutagenic studies and transient co-transfections experiments showed that SRF alone is not sufficient to transactivate the *CFTR* gene. Upon some mutations of the *CFTR*-CArG-like element, promoter activity is severely decreased, potentially implying YY1 as a co-repressor. Given the YY1 well-defined role in the transcriptional regulation of some SRE-dependent promoters (30–33), we explored the putative role of YY1 on the *CFTR* promoter activity and demonstrated functional interplay between this factor and SRF. Finally, by stringent *in silico* structural analysis, we identified additional multiple near consensus CArG sites within the highly conserved promoter and intronic regions of the *CFTR* gene. We also documented the existence of SRF-containing protein complexes on numerous predicted *CFTR* CArG-like elements. Taken together, the data obtained classify *CFTR* as a novel SRF target gene, subject to modest but significant SRF activation, and open the gate to further investigate how SRF may be involved in the regulation of *CFTR* gene expression.

MATERIALS AND METHODS

Cell culture

Human bronchial epithelial cells, Beas2B and A549 expressing endogenous CFTR were kindly provided by Dr Marc Chanson, Department of Pediatrics, Laboratory of Clinical Investigation, Switzerland. Beas2B and A549 cells were maintained in high glucose DMEM (4500 mg/l D-Glucose, Invitrogen Corporation) supplemented with 10% fetal bovine serum (FBS) (Eurobio, France) and 5 mM L-glutamine. C2C12 myoblasts were grown in DMEM supplemented with 10% FBS and 5 mM L-glutamine. All cell cultures, supplemented with 100 U ml^{-1} penicillin and 100 mg ml^{-1} streptomycin, were maintained at 37°C under 5% CO_2. As positive or negative controls for the different assays, other cells used in this study included colon adenocarcinoma Caco-2 cell line (ECACC) with functional CFTR (34,35) and normal monkey kidney fibroblast-like COS-7 cell line (ATCC) which does not express CFTR (36,37); all were maintained in DMEM supplemented with FBS and were incubated in the same conditions as above.

Plasmids constructs

The original luciferase expression vector pGL3-Basic containing the wild-type human *CFTR* minimal promoter was described previously (12). To further study the putative composite *cis*-acting element located at –108 from the major transcription initiation site of the human *CFTR* promoter (38), the *CFTR*-CArG-like motif was either mutated in a consensus CArG box or in a degenerated motif. Mutations were introduced into the WT-pGL3 plasmid using an oligonucleotide-directed mutagenesis system (QuickChange™Site-Directed Mutagenesis Kit, Stratagene) according to the manufacturer's instructions. Mutagenesis primers are depicted in Table 1. The presence of mutations and sequence fidelity were verified by dideoxynucleotide sequencing. For each introduced mutation the loss or the improvement of transcription factor binding activity was checked by *in vitro* assays. The 3xSRE-fos TATA-luciferase reporter construct was kindly provided by R. A. Hipskind, Institut de Genetique Moleculaire, Montpellier, France. Expression vectors encoding either human wild-type SRF, the pHiv-SRF or SRF dominant-negative form deleted of an essential part of DNA-binding domain (DBD), the pHiv-DN, were generously given by D. Trouche, Laboratoire de Biologie Moleculaire Eucaryote, Toulouse, France. Another dominant-negative SRF mutant, pHiv-DBD, was constructed by PCR amplification of SRF fragment spanning the DBD flanked by HindIII and HincII sites to facilitate cloning into expression vector. The PCR was performed using pHiv-DBD-SRF primers (listed in Table 1), 10 ng of SRF expression vector, 200 μM of each dNTP, 0.5 μM of each primer and 1.5 U *Taq* DNA polymerase (Perkin Elmer, Inc.) in a 1× reaction buffer provided by the manufacturer. TranSilent human control siRNA vector and TranSilent™ human SRF siRNA vector (catalog no. SR1038) were purchased from Panomics. Expression vectors encoding either pCMV-YY1 or pcDNA3-YY1 were generously provided by E. Seto, E. Bonnefoy and A. Moustakas, respectively.

Transient transfections

Cells were seeded at a density of 200 000 cells/2 ml of medium and plated in 6-well dishes (NUNClone®, Merck-Eurolab, Inc.). After a culturing period of 24 h, cells were transfected with PolyFect® transfection reagent (Qiagen Corporation,

Table 1. Sequences of oligonucleotides

	Primer sequence	Annealing temperature
RT–PCR primers (5′→3′)		
Hprt human forward	TGT AAT GAC CAG TCA ACA GGG	52°C
Hprt human reverse	TGA CCA AGG AAA GCA AAG TCT G	
SRF forward	CTA CCA GGT GTC GGA GTC TGA	52°C
SRF reverse	CCA GAT GAT GCT GTC AGG AAC A	
CFTR external primers forward 729	TTT CGT GTG GAT CGC TCC TT	57°C
CFTR external primers reverse 1487	TCC AGC AAC CGC CAA CAA CT	
CFTR external primers forward 757	GCA CTC CTC ATG GGG CTA ATC T	59°C
CFTR external primers reverse 1436	TTC AGG ACA GGA GTA CAA AGA A	
Expression vector construct primers (5′→3′)[a]		
pHiv-DBD-SRF forward	**AAG CTT** ATG AGC GGG GCC AAG CCG GG	65°C
pHiv-DBD-SRF reverse	**GTC AAC TCA** GAA CGC CGG CTT CAG TGT G	
Chromatin immunoprecipitation primers (5′→3′)		
Negative control		
β-Globin forward	GCT TAC CAA GCT GTG ATT CC	
β-Globin reverse	AAG CAA TAG ATG GCT CTG CC	54°C
Positive control		
β-Actin forward	ATG CTG CAC TGT GCG GCG AA	
β-Actin reverse	GTC GCG CCG CTG GGT TTT AT	64°C
Target sequence *CFTR* minimal promoter		
CFTR-CArG-like forward	GGC TCG AGG CTG GGA GTC AGA ATC GG	
CFTR-CArG-like reverse	TTC CAT GGT CTC TCG GGC GCT GGG GT	70°C
Target sequence: CArG located at 2373 bp of the *CFTR* promoter		
CArG3 forward	GTT AAA GCT CTG AAT AAT GC	54°C
CArG3 reverse	CAC ACA TGT ACA TAG GAA GA	
Site-directed mutagenesis primers (5′→3′)[b]		
C2	GAA AGC CGC TAG A***C***C AAA TTT GGG GCC GGA CC	
C3	GAA AGC CGC TAG A***C***C AAA T**A**T GGG GCC GGA CC	
C4	GAA AGC CGC TAG A***C***C A***T***A TTT GGG GCC GGA CC	
C5	GAA AGC CGC TAG A***C***C A***T***A T**AA** GGG GCC GGA CC	
D1	GAA AGC CGC TAG AGC AAA TIT G***T***G GCC GGA CC	
D2	GAA AGC CGC TAG AGC A***CG*** TTT G***T***G GCC GGA CC	
D3	GAA AGC CGC TAG AGC AAA T**A**T G***T***G GCC GGA CC	
D4	GAA AGC CGC TAG AGC A***CG*** T**A**T G***T***G GCC GGA CC	

[a]Bold type indicates the restriction sites: HindIII and HincII.
[b]Bold and italicized type indicates mutated nucleotides.

France) according to the manufacturer's recommendations. For transient transfection, we used 1.8 μg of plasmid reporter and 0.2 μg of internal control pRL-SV40 containing *Renilla* luciferase (Promega Corporation). The pGL3-Basic vector lacking both eukaryotic promoter and enhancer sequences was used as a negative control. After 48 h, the luciferase activity was evaluated with the Dual Luciferase Reporter Assay System (Promega Corporation), as described previously (12). Luminescence measurements were performed on a Luminoskan Ascent luminometer (ThermoLabsystem Corporation, France). Firefly luciferase activity was normalized to *Renilla* luciferase activity. All luciferase activities represent at least three independent experiments with each construct tested in triplicate per experiment. Luciferase activity data are expressed as the means ± SD computed from the results obtained from each set of transfection experiments. To minimize the possibility of errors in DNA amplification, at least two independently constructed clones were tested. For co-transfection assays, unless otherwise indicated, 1.8 μg of luciferase reporter and 1–2 μg of each expression vector were used. Transfection with siRNA was performed using Lipofectamine 2000 (Invitrogen) with 2.5 μg of siRNA. The cells were transfected with *CFTR* promoter plasmid reporter, and luciferase activity was determined as described above. Aliquots of cell lysates were used for western blotting to confirm the specificity and level of SRF protein knockdown.

Preparation of whole cell proteins, nuclear extracts and recombinant protein production

For the CFTR immunodetection analyses, Beas2B, A549, C2C12, COS-7 and Caco-2 cells were treated with 5 mM sodium phenylbutyrate, which has been previously reported to increase CFTR (39) and scraped into lysis buffer (50 mM Tris–HCl, 1% NP-40, 40 mM beta-glycerophosphate and 120 mM NaCl) supplemented with protease inhibitors [1 mM phenylmethylsulfonyl fluoride (PMSF), 1 mM DTT, and 1 μg/μl aprotinin, leupeptin and pepstatin]. Nuclear extracts were prepared using the Nuclear extraction kit according to the procedure recommended by the supplier (Panomics, Ozyme, France). Protein concentrations were determined using the Bio-Rad Protein Assay kit with BSA as a standard, based on the classical Bradford method. The pGEX-SRF plasmid, a generous gift from D. Trouche (Laboratoire de Biologie Moleculaire Eucaryote), was used for protein expression. GST–SRF fusion protein was purified from *Escherichia coli* as described previously (40). The purity and concentration of protein samples were estimated by SDS–PAGE.

Electrophoretic mobility shift assay (EMSA) and supershifts

Oligonucleotides probes were synthesized corresponding to *CFTR* CArG-like element and mutant versions in which the

Table 2. Oligonucleotides used in EMSA analysis

Oligonucleotides (5′→3′)	
SRE[a]	GG ATG TCC ATA TTA GGA CAT CT
GATA[b]	CGG CCC CTA TCG GGA CGC AGC ACC TGG CGC CGA
WT[c]	GAA AGC CGC TAG AGC AAA TTT GGG GCC GGA CCA GGC AGC
C1[d,e]	GAA AGC CGC TAG AGC AAA T***A***T GGG GCC GGA CCA GGC AGC
C2[e]	GAA AGC CGC TAG A***C***C AAA TTT GGG GCC GGA CCA GGC AGC
C3[e]	GAA AGC CGC TAG A***C***C AAA T***A***T GGG GCC GGA CCA GGC AGC
C4[e]	GAA AGC CGC TAG A***C***C A***T***A TTT GGG GCC GGA CCA GGC AGC
C5[e]	GAA AGC CGC TAG A***C***C A***T***A T***AA*** GGG GCC GGA CCA GGC AGC
D1[f]	GAA AGC CGC TAG AGC AAA TTT G***T***G GCC GGA CCA GGC AGC
D2[f]	GAA AGC CGC TAG AGC A***CG*** TTT G***T***G GCC GGA CCA GGC AGC
D3[f]	GAA AGC CGC TAG AGC AAA T***A***T G***T***G GCC GGA CCA GGC AGC
D4[f]	GAA AGC CGC TAG AGC A***CG*** T***A***T G***T***G GCC GGA CCA GGC AGC
CArG 1	AAC ATT CAT CCA TGT CCT TAT GTG GCT TGT AGT TCA TTA
CArG 2	TTG TCA TAA TAA TTG GCA TAT ATG GTA AGT GAC CAA CAA
CArG 3	TTT ATT TCT ACC AAA ACA AAT TTG GGC TGT AAT GTT TTA
CArG 4	TTA ACT GAG CTT GGC CCA CAT ATG GTG TAG TGA CAT GCT
CArG 5	CAA CTG TCA GGT AGC AAT ATA TGA TGG AAG AAG CAT GTA
CArG 6	ATT TCT ATT TTG TTC CTA TAT TAG GCC AAG GAG AGG TGG
CArG 7	TTG AAC TGA ACT GGC CAT TTA TGG GAA AGG TCA CTG GGT
CArG 8	ATC CTT GGT TGT AAC CTA TAA AAG GAG ACA GAT TCA AGA
CArG 9	AAC CTG GAA GAT CTC CCA AGT ATG GGG GAA GGT TTC ACC
CArG 10	CCA AAT GAT ACT TGA CCA AAT TTG TCC CTT TGG CTT GTT

Bold and italicized type indicates mutated nucleotides. The CArG boxes in the *CFTR* minimal promoter are shaded. The underlined nucleotides indicate the *in silico* predicted CArG elements in the non-coding regions of the *CFTR* gene.
[a]c-*fos* consensus SRE (56).
[b]Oligonucleotide for competition assay, the GATA and E-box sequences are boxed (85).
[c]CArG-like box located in the human minimal *CFTR* promoter region.
[d]CArG-like box located in the human minimal *CFTR* promoter region containing the naturally occurring variant [−102T>A] (12).
[e]Consensus CArG box with minimal *CFTR* promoter flanking sequences.
[f]Mutated CArG box with minimal *CFTR* promoter flanking sequences.

CArG motif was either mutated in a consensus box or disrupted. The oligonucleotide sequences were listed in Table 2. Single-stranded complementary oligonucleotides containing the studied sequences were annealed, end-labeled with [γ-^{32}P]ATP (5000 Ci/mmol) and purified as described previously (12). Mobility assay conditions were specifically optimized for binding of SRF. The binding reaction was carried out in a total volume of 20 µl containing 2 ng (∼30 000 c.p.m.) of the labeled probe, 10 µl of binding buffer (2×), 0.25 µg poly(dI–dC) (Amersham Pharmacia) used as a non-specific competitor, 5–12 µg of nuclear extracts and 100–1000 ng of GST–SRF fusion chimera protein. For EMSA competition and antibody interference assays, proteins were incubated with either cold specific competitors (WT and SRE oligonucleotides, see Table 2), unspecific competitor (GATA oligonucleotide, see Table 2) or purified antibodies (anti-SRF: sc-335X; anti-YY1: sc-1703X or anti-HA, Santa Cruz, Biotechnology Inc., TEBU, France) for 20 min before addition of labeled probes. After incubation of 30 min at room temperature, complexes were resolved on 5% acrylamide: bisacrylamide (29:1) native gel containing 0.5× TBE at 26 mA for 1 h.

Formaldehyde cross-linking and chromatin immunoprecipitation

Beas2B and A549 cells proteins were cross-linked to DNA by adding formaldehyde to a final concentration of 1% for 10 min at 37°C. The fixed cells were prepared for immunoprecipitation using the protocol of ChIP assay kit (Upstate Biotechnology Inc., Euromedex, France) with minor modifications. Cells were resuspended in 1 ml cold phosphate-buffered saline (PBS), pelleted by centrifugation and lysed in 800 µl of SDS lysis buffer (1% SDS, 10 mM EDTA, 50 mM Tris–HCl, pH 8.1) containing protease inhibitors (1 mM PMSF, 1 µg/ml aprotinin and 1 µg/ml pepstatinA). After incubation on ice for 10 min, the cross-linked chromatin was sheared by sonication at the following conditions eight times for 10 s at 40% of maximum power and diluted 10-fold in ChIP dilution buffer (0.01% SDS, 1.1% Triton X-100, 1.2 mM EDTA, 16.7 mM Tris–HCl, pH 8.1 and 167 mM NaCl) with protease inhibitors. Aliquots containing 20 µl of each aliquot were used as a control to show total input DNA. The chromatin solution was precleared with 80 µl of salmon sperm DNA/protein A agarose-50% slurry (Upstate Biotechnology Inc.) for 1 h at 4°C under agitation, and subsequently incubated at 4°C on a rotating stand overnight with either 3 µl of anti-SRF antibody (sc-335X, Santa Cruz, Biotechnology Inc.) or an irrelevant antibody (anti-HA). Immune complexes were precipitated by the addition of 60 µl of salmon sperm DNA/protein A agarose and incubated at 4°C for 1 h and low speed spinning. Precipitates were washed once with 1 ml of low salt buffer, once with high salt buffer, once with LiCl buffer and twice with 1× TE, according to the manufacturer's recommendations (Upstate Biotechnology Inc.). The cross-links were reversed by the addition of 20 µl of 5 M NaCl and incubation at 65°C overnight. The samples were treated with proteinase K, phenol–chloroform extracted, ethanol precipitated and resuspended in 30 µl of sterile water. PCR analysis was carried out using primers from different regions of the human *CFTR* promoter and as additional controls from promoter regions of a number of genes that are either silent (β-globin) or having at least one functional CArG element (β-actin). The sequences of PCR primers are listed in Table 1. After 45 cycles of amplification, PCR products were separated on 1.8% agarose gels and visualized by ethidium bromide staining and UV transillumination.

Reverse transcriptase–PCR

Total RNA from epithelial cells (Beas2B and A549), myoblasts (C2C12) and fibroblasts (COS-7) was isolated using the SV Total RNA Isolation System® (Promega, France). Reverse transcription was performed with 3 µg of total RNA, 300 ng of random hexamers (Invitrogen Corporation), 10 mM dNTPs, 1 µl of RNasin RNase inhibitor (Promega), 2 µl of DTT at 0.1 M, 4 µl of first strand buffer (Invitrogen), 200 U of M-MLV RT (Invitrogen) and nuclease-free water (Promega) in a final reaction volume of 20 µl. For each RNA template, a control reaction without RT was included. For each RT reaction condition, an H_2O no-template reaction was included as an additional negative control. The reaction mixture was incubated first for 10 min at 25°C, then 40 min at 42°C; this was followed by a heat inactivation step of 72°C for 3 min. Aliquots containing 1 µl of the cDNA synthesis reaction mixture were used for PCR analyses. The expression level of *SRF* mRNA was analyzed by PCR amplification of the endogenous *Hypoxanthine PhosphoRybosyl-Transferase* (*HPRT*) gene used as internal control. Amplification mixture

included either 10 pmol of each *SRF*-specific primer or 10 pmol of each *HPRT*-specific primer, 1.5 U of AmpliTaq polymerase (Applied Biosystem Corporation) and nuclease-free water (Promega) in a 25 µl volume. Amplification was performed with an initial denaturation step at 95°C for 5 min, followed by 35 cycles of 30 s of 95°C denaturation, 60 s of 52°C annealing and 2 min extension at 72°C. Amplification of *CFTR* was performed as described previously (41). The RT–PCR products were separated on an 8% non-denaturing polyacrylamide gel, stained with ethidium bromide. To ensure that the sequence of cDNA products derived from both *SRF* and *CFTR* RT–PCR analyses correspond to respective published sequences, the cDNA bands were purified and prepared for dideoxy DNA sequencing. Controls included RNA preparations from monkey kidney fibroblasts (COS-7), which are negative for CFTR expression (36,37).

Western blot analysis

Twenty-five microgram protein extracts (except where otherwise indicated) were resolved on a 10% (except where otherwise indicated) SDS–polyacrylamide gel and transferred onto a nitrocellulose membrane (except where otherwise indicated). All membranes were Ponceau S stained to ensure sample integrity. Briefly, the membranes were blocked with 5% skim milk in PBS supplemented with 0.01% Tween-20 and incubated with diluted primary antibodies in 5% skim milk (1:5000 diluted anti-SRF Abs: sc-335X and sc-25290X purchased from Santa Cruz; 1:1000 diluted anti-CFTR Ab: 24.1 from R&D System; 1:2500 diluted anti-β-actin antibody: AC-15 from Sigma, 1:2500 diluted anti-β-tubulin antibody: T6074 from Sigma) overnight. The membranes were then washed and incubated with an appropriate horseradish peroxidase (HRP) conjugated secondary antibody at 1:15 000 in PBS-5% milk. The membranes were reacted with chemiluminescence reagent ECL (Roche Diagnostic) as described by the manufacturer and subsequently exposed to Biomax photographic film (Kodak Corporation). The protein levels of the actin housekeeping gene (except where otherwise stated) were assayed for internal control of protein loading.

Indirect immunofluorescence

A549, Beas2B, C2C12 and COS-7 cells were plated on Lab-Tek™II CC2™ Chamber Slide™ systems (Nalge Nunc) 1 day before immunohistochemical analysis. The cells were fixed and permeabilized in 4% paraformaldehyde and 0.1% Triton X-100, respectively, for 20 min durations at room temperature. Non-specific binding sites were blocked with 1% BSA in PBS for 1 h. The cells were subsequently incubated with primary antibodies diluted in 1:100 in PBS–BSA. Antibodies used included, the clone L12B4 (Upstate biotechnology), an anti-CFTR antibody known to recognize human, rat, mouse and bovine CFTRs (42) and the H-300 or the A11 anti-SRF antibody (sc-13029 and sc-25290, Santa Cruz). The specificity of the anti-CFTR antibody has been described previously (43,44) and was also verified by using a CFTR-positive human Caco-2 cell line (34,35). For nuclear counterstaining, DAPI (sc-3598, Santa Cruz) was applied at a concentration of 1:5000. Cells were then washed with PBS–BSA and incubated with either donkey anti-rabbit fluorescein isothiocyanate-conjugated (FITC) or donkey anti-mouse Cy3™ conjugated secondary antibody (Jackson ImmunoResearch Laboratory Inc.) diluted 1:200 for 1 h at room temperature. Cells were washed twice with PBS–BSA, once with PBS, and mounted with Dakocytomation fluorescent mounting medium (Dakocytomation). Indirect immunofluorescence was examined with an inverted Leica DMR microscope (Leica Microsystemes SAS). Final images were further processed using Adobe Photoshop 7.0 software.

Statistical analyses

Transfection data are expressed as the mean ± SE. Paired comparisons were made using student's *t*-test. Data were considered statistically significant at $P < 0.05$. All graphical data and statistical analyses were generated with GraphPAD Prism software (Version 3.0). Densitometric analysis was performed using computerized densitometry and ImageQuant^{TL} v.3.0 software (Amersham Biosciences). Densitometric values for both transcript and protein bands were determined in areas of equal size and are reported in normalized arbitrary units relatives to the expression of either *HPRT* gene or actin protein set to 1 (except where otherwise indicated).

Computational analyses

The computer program ConSite (http://www.phylofoot.org/), particularly suited to the analysis of large genomic sequences, was used to identify putative CArG binding sites within the promoter and intronic regions of the human *CFTR* gene. The algorithm AliBaba 2.1 (http://www.alibaba2.com/) was then used to verify these predictions and minimize false negatives or positives. To prevent a possible bias introduced by palindromic or internally repetitive *cis*-regulatory elements, overlapping matches, including on opposite DNA strands, were defined as a single match.

To assess the importance of the putative CArG elements identified in the non-coding regions of the human *CFTR* gene, we performed multiple sequence alignments. The human, cynomolgus, gibbon, squirrel monkey, rabbit, pig, sheep and cow sequences were aligned using the ClustalW global alignment tool (http://clustalw.genome.ad.jp/) (45). The gap open and extension penalties were set at 15 and 6.66, respectively, and sequence delay divergence of 30% with a DNA transition weight of 0.5 was used.

RESULTS

CFTR minimal promoter region encompassing the CFTR-CArG-like element is remarkably conserved

To search the *cis*-acting elements involved in the *CFTR* gene expression regulation, we previously performed an *in silico* search for transcription factor binding sites (46), and reported that the human minimal *CFTR* promoter contains a CArG-like motif, which is localized –108 bp upstream of the major transcription initiation start site (38). Because so far all described CArG-box elements were found in the regulatory regions of immediate early genes (47) and in muscle-specific genes (22), we confirmed our first binding site prediction by using two other algorithms, AliBaba (http://www.alibaba2.com/) and ConSite (http://clustalw.genome.ad.jp/). As shown in Figure 1A, the *CFTR*-CArG-like element sequence

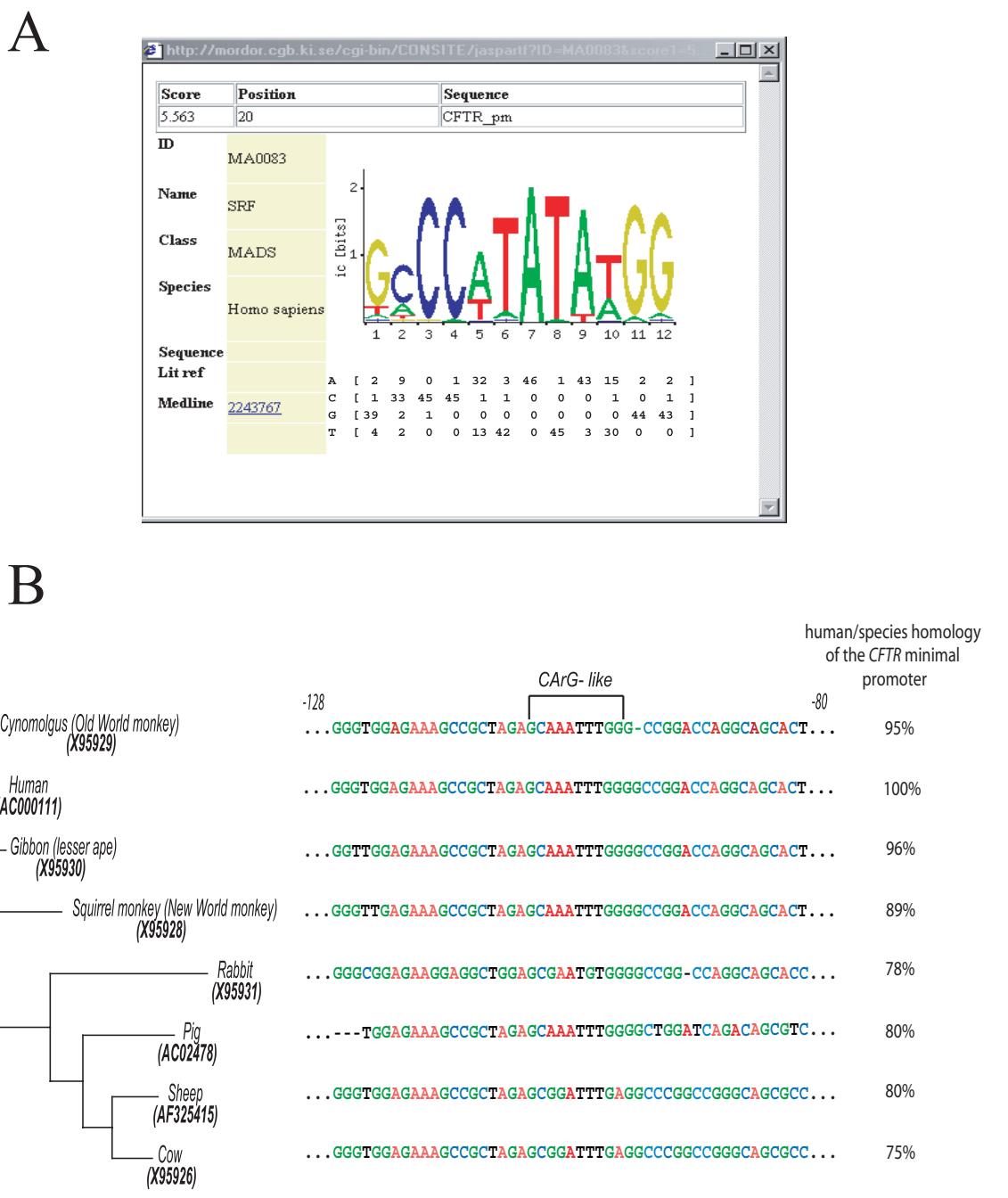

Figure 1. Cross-species comparison of the *CFTR*-CArG-like element. (**A**) Visualization of consensus CArG binding site: pop-up window containing information about SRF transcription factor obtained from *in silico* analysis performed with the ConSite tool. (**B**) Detailed alignment view of the CArG-like element-including region of human *CFTR* minimal promoter with seven orthologous sequences: Cynomolgus, Gibbon, Squirrel Monkey, Rabbit, Pig, Sheep and Cow. Dashes indicate gaps that were introduced to maximize alignment. Each sequence is represented by a classical text representation with each nucleotide assigned its own color (A is colored in red, C in blue, G in green and T in black). The numberings above the Cynomolgus sequence are indicated according to the major human transcription initiation site. In the left panel, the phylogenetic relationships between the different species are illustrated in a rooted tree, directly derived from ClustalW program. In the right panel, human/species homologies are indicated. The accession number of each *CFTR* genomic sequence is indicated below each species name, in brackets and bold characters. The human *CFTR*-CArG-like motif is noted above the Cynomolgus sequence.

(***G***C(A/T)$_6$GG) diverges slightly at the 5′ from the published SRF consensus sequence (**C**C(A/T)$_6$GG) (22,37). However, this divergence is similar to that observed in the smooth muscle-gamma-actin promoter which has been demonstrated to bind SRF (48).

To assess the putative functional importance of *CFTR*-CArG-like binding site, we used an orthogonal approach of deducing regulatory elements by considering orthologous *CFTR* minimal promoter regions from several mammalian species representing the Primates, Artiodactylia and

Lagomorpha orders. Comparison of human/species homologies was carried out using ClustalW multiple *CFTR* sequence alignments according to the numerous alignment parameters described previously (49). Consistent with previous studies (50,51), we showed that the human minimal *CFTR* promoter is remarkably conserved across the orders studied (Figure 1B, right panel). We found that the *CFTR*-CArG-like element is conserved within all the Primates species studied and also within the pig while, within the sheep, cow and rabbit species, some substitutions occur in the middle of the CArG-like motif (Figure 1B). These data are consistent with previous *CFTR* promoter phylogenetic work that identified two types of regulatory elements: some are conserved between species, such as a non-consensus CRE at positions –0.1 kb relative to ATG and some are species-specific elements, such as a 300 bp purine.pyrimidine (Pu.Py) stretch that is present only in rodents (50).

Bronchial epithelial expression of SRF

Because we could not previously identify SRF binding to the *CFTR* CArG-like element, even though an anti-SRF antibody had been used (12), we asked whether SRF, mainly described as highly expressed in muscle cells, was also present in epithelial cell lines. To measure the expression levels of *SRF* mRNAs, we used a RT–PCR-based procedure previously described by Davis *et al*. (52). As reverse-transcribed control, the *Hypoxanthine PhosphoRybosyl-Transferase* (*HPRT*) housekeeping gene was amplified. Amplification of *SRF* from bronchial epithelial cells and myoblasts yielded a fragment of the same size, 651 bp (Figure 2A), as that of the full-length *SRF* transcript produced by RT–PCR from human hearts (52). The 453 bp band corresponding to *SRF* lacking exon 5 (SRFΔ5) was only detected in the C2C12 myoblast line (Figure 2A). To ensure that these bands were not the result of a PCR artifact or genomic contamination of samples, negative controls such as exclusion of RT or RNA during cDNA synthesis were included in each assay. As expected, no PCR product appeared when either RT or the template was omitted (Figure 2A). Densitometric analysis revealed that bronchial epithelial cells contained an appreciable amount of *SRF* mRNA. Nuclear extracts from A549, Beas2B and C2C12 cells were electrophoresed and then assayed by western blotting with anti-SRF antibody reported to recognize all four isoforms of the protein (52). As shown in Figure 2B, we found that robust expression of a 67 kDa band, that based on molecular mass, corresponds to full-length SRF (SRF-FL) in all of the cell lines examined. Consistent wit RT–PCR analysis, a 57 kDa band corresponding to SRFΔ5 was only detected in the C2C12 myoblast line. As a control, we checked the β-actin levels (Figure 2B). Densitometric analysis of western blot revealed no apparent difference in the expression level of SRF proteins between the myoblasts and epithelial cells (Figure 2B). In subsequent western blot analyses in which parallel blots were probed with only the secondary antibody, no band was detected (data not shown), thus confirming that these bands are indeed specific for SRF. As further evidence, A549, Beas2B and C2C12 cells express relatively large amounts of SRF, the cell lines were assessed by indirect immunofluorescence labeling. A similar staining pattern was noted in the bronchial epithelial cells and myoblasts

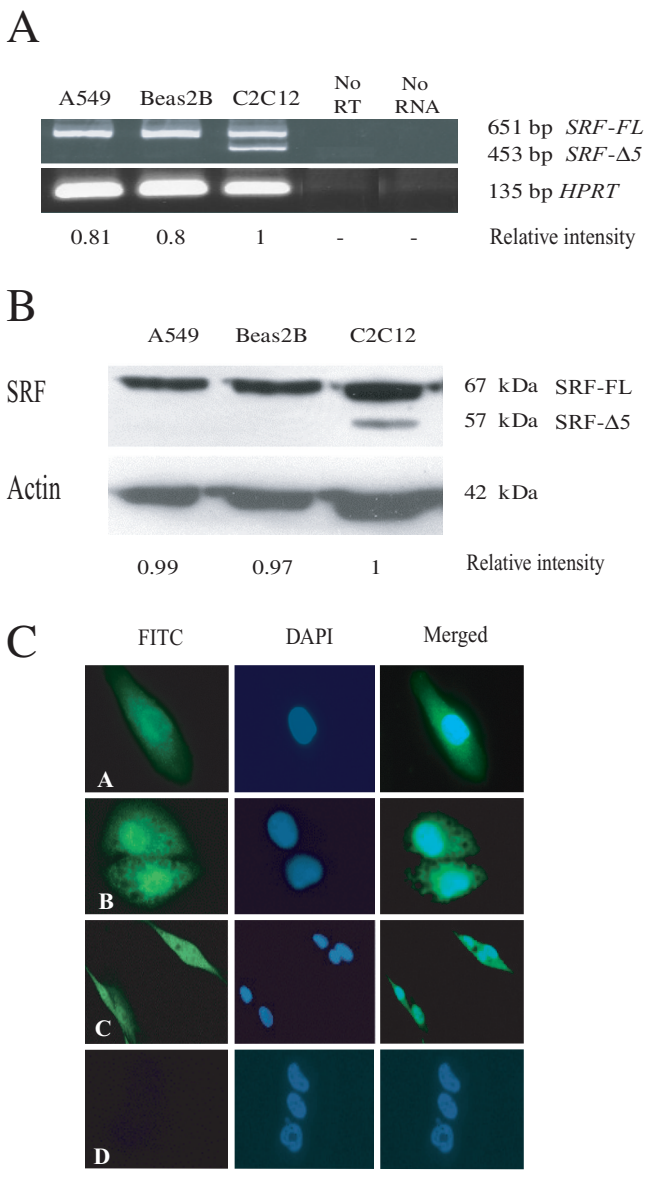

Figure 2. Bronchial epithelial expression of SRF. (**A**) Detection of *SRF* and *HPRT* transcripts from both bronchial epithelial and myoblast cell lines by RT–PCR analysis. Total RNAs isolated from A549, Beas2B and C2C12 cells, as indicated, were reverse transcribed with random hexamers and PCR amplified with *SRF* or *HPRT* primers. Amplified products were directly stained with bromide ethidium on non-denaturing polyacrylamide gel. Expected size of PCR products is given at left of each transcript. Negative controls are noted as follow: No RT for the absence of reverse transcriptase and No RNA for an H_2O no-template reaction. Densitometric analysis of SRF bands intensity was performed with relative HPRT mRNA expression in C2C12 myoblasts. (**B**) Western blot analysis of nuclear extracts prepared from both epithelial and myoblast lines. Each extract (25 μg) was separated by SDS/PAGE (10%) and western blotted using an anti-SRF Ab. Relative mass, in kilodaltons, is indicated alongside. As a control for proteins loading in SDS–PAGE, an anti β-actin Ab was used in western blot. Numbers below the β-actin panel indicate densitometric values of the total SRF bands normalized over the corresponding β-actin bands and expressed relative to the C2C12 controls bands, which are set to 1. (**C**) The A549, Beas2B and C2C12 cells (rows A, B and C, respectively) were grown on coverslips, fixed and subjected to indirect immunofluorescence with anti-SRF Ab. Left panel, cells were stained with FITC-conjugated secondary antibody (green). Middle panel, cells were counterstained with DAPI (blue) for nuclear staining. Right panel, shown is merge of SRF immunostaining and DAPI. Row D, background immunofluorescence obtained in the absence of the primary antibody.

(Figure 2C, rows A–C). The nuclei have been stained blue with DAPI. As negative control, no staining was detected when the primary antibody was omitted (Figure 2C, row D). Consistent with other studies reporting that SRF is ubiquitously expressed in a variety of cell types (26,27,53), our SRF expression studies demonstrated that human SRF gene is expressed in bronchial epithelial cells.

SRF binds the CFTR-CArG-like element

Because the CArG box is not only found in the regulatory regions of many muscle-specific genes but also located at the center of other SREs (54) and forms the core binding site for SRF (55), we have attempted to determine whether or not SRF binds to the *CFTR*-CArG-like element sequence. We performed two series of bandshift experiments. First, we incubated the ^{32}P-labelLed WT oligonucleotide corresponding to *CFTR*-CArG-like element sequence (as indicated in Table 2) with bacterially expressed SRF. As shown in Figure 3A (lane 3), EMSA revealed a recombinant SRF–WT duplex. As shown in Figure 3A (lane 5), bands defined as the *CFTR*-CArG-like-SRF complex disappeared when 100-fold molar excess of specific competitor containing the consensus SRE motif, derived from human *c-fos* promoter (56), was added. In contrast, competition by an irrelevant oligonucleotide (noted UC) did not appear to significantly alter the complex suggesting specificity of binding (lane 6). To confirm precisely the identity of protein binding in the minimal *CFTR* promoter (from –121 to –83 bp), bacterially expressed SRF was preincubated with anti-SRF antibody before incubation with ^{32}P-labelled probe. As shown in Figure 3A (lane 4), bands corresponding to *CFTR*-CArG-like-SRF complex disappeared, and more slowly migrating bands appeared when anti-SRF antibody was added. To verify the antibody specificity, control experiments were performed either in the absence of the SRF protein (Figure 3A, lane 7) or in the presence of an irrelevant antibody (Figure 3A, lane 8). These results demonstrate that the *CFTR*-CArG-like element is a bona fide SRF-binding site. Second, we performed additional EMSA with the WT oligonucleotide, as main binding target, and nuclear extracts from both epithelial and muscle cells (Figure 3B). While three nucleoprotein complexes were formed from nuclear extracts of Beas2B and C2C12 cells on the WT probe, five complexes were detected from A549 cells. Each nuclear protein complex was designated by an upper case relative to nuclear lysate followed by a Roman numeral indicating its position into the gels. The binding specificity of the different complexes was examined by competition analyses with both specific and non-specific unlabeled oligonucleotides (Figure 3B, lanes 2–4). Although a few non-specific binding activities were observed, complexes BII, BIII, AIII, AV, CI, CII and CIII were efficiently competed with an excess of both WT and *c-fos* SRE unlabeled specific competitors indicating binding specificity (Figure 3B, lanes 2 and 3, respectively). Control experiments including an irrelevant oligonucleotide did not reveal any change in electrophoretic profiles (Figure 3B, lanes 4). To evaluate whether the SRF protein contributes to the formation of nucleoprotein complexes interacting with the CFTR-derived SRF site, we used a specific antibody against the SRF protein. Although the incubation with the anti-SRF antibody apparently failed to give any discrete supershift from various sources of nuclear proteins, a significant decrease of specific complexes was observed (Figure 3B, lanes 6). This effect seemed to be specific because none of these nuclear protein complexes was supershifted or abolished when a non-specific antibody was used (Figure 3B, lanes 7). Control experiments containing only the anti-SRF antiserum and the radiolabeled WT oligonucleotide did not reveal any binding activities (Figure 3B, lanes 8). In addition, supershift assays performed with the radiolabeled *c-fos* SRE oligonucleotide instead of the WT probe showed that bands corresponding to SRE–SRF complex disappeared and more slowly migrating bands appeared (Figure 3B, lane 10). The absence of supershift for specific WT binding complexes (Figure 3D, lanes 6) may be explained if the epitope recognized by the anti-SRF antibody is part of (or located near) the *CFTR*-CArG-like DNA-binding site. Antibody binding would compete DNA binding, resulting in a significant decrease or total disappearance of CArG-like complexes rather than in supershifted complexes. Alternatively, if the interaction between the *CFTR*-CArG-like DNA-binding site and the SRF protein is insufficiently strong, it could be not as stable as the one observed with the SRE probe (Figure 3B, lane 10) to be detected as a supershift in gel retardation assays. On the one hand, other DNA-binding proteins that are potentially part of this complex could interfere with the antibody's access to SRF protein. Taken together, these EMSA studies establish SRF-binding CArG-like box within the minimal promoter of the human *CFTR* gene.

SRF binds the CArG-like motif of the *CFTR* minimal promoter within intact chromatin under physiological conditions

Although there is extensive evidence that SRF can bind to CArG-like elements in *in vitro* assays and that it is involved in transcriptional regulation through CArG elements in reporter assays in cultured cells with a typical epithelioid morphology (53), there is a lack of direct evidence for involvement of SRF in transcription of the endogenous *CFTR* gene within the context of intact chromatin. To directly address whether SRF also binds *in vivo*, ChIP was carried out in bronchial epithelial cells. For this purpose, DNA-binding proteins of Beas2B epithelial cells were covalently linked to genomic DNA by treatment of the cells with formaldehyde. Cross-linked chromatin was immunoprecipitated with either specific or irrelevant antibodies, anti-SRF and anti-HA, respectively. The precipitated chromatin DNA was then purified and amplified by PCR with specific primers of the target sequences (Table 1). The promoter of β-*globin* gene, which lacks CArG elements, was used as negative control (Figure 4, row A). The skeletal β-*actin* promoter sequence, which contains at least a consensus SRF-binding site, was used as positive control (Figure 4, row B). As expected, PCR signals were obtained when the DNA/protein adducts were immunoprecipitated with an anti-SRF antibody from both Beas2B (Figure 4, rows B and C, lane 1) and A549 (data not shown) epithelial cell lines. In contrast, the negative controls, in which immunoprecipitation was performed with an irrelevant antibody (Figure 4, rows A–C, lane 3) or without antibody (Figure 4, rows A–C, lane 2), did not show any PCR signal. These results were reproduced in several independently

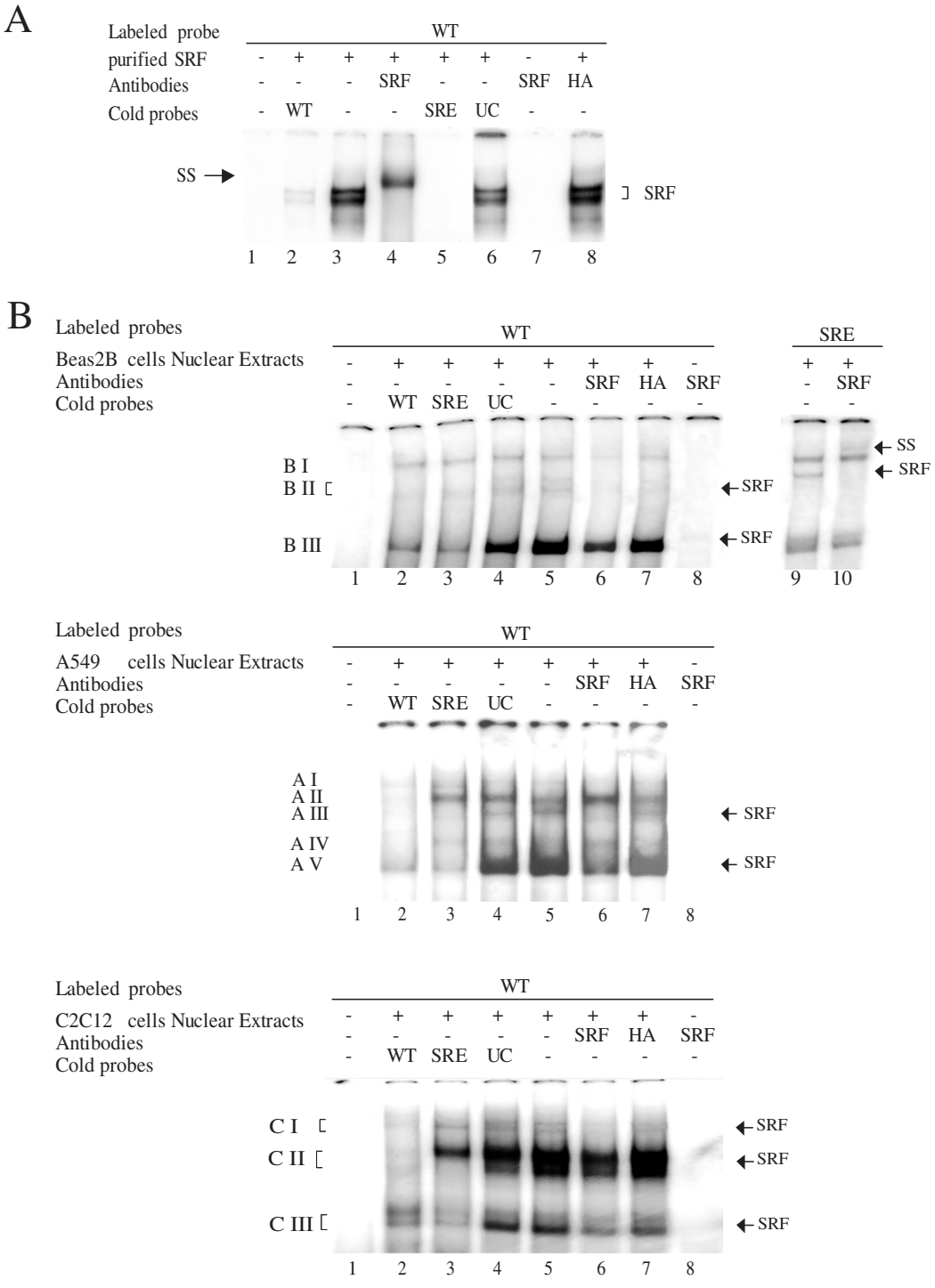

Figure 3. SRF is a component of *CFTR*-CArG-like binding complexes. (**A**) EMSAs were performed with a radiolabeled oligonucleotide encompassing the studied *CFTR*-CArG-like motif (noted WT, see Table 2) and bacterially expressed SRF (lane 3). Competition assays were carried out using a 100-fold molar excess of two specific competitors, noted WT and SRE (lanes 2 and 5, respectively). *UC* (lane 6) indicates unspecific competitor that is used as negative control. Supershift assays were carried out using either a specific antibody (lane 4) or an irrelevant antibody (lane 8). The arrow SS indicates the Ab-supershifted complex. Neither the retarded nor the supershifted complexes were found when the ^{32}P-labeled WT double-stranded oligonucleotide was incubated either only with the binding buffer (lane 1) or with specific anti-SRF antibody in the absence of purified SRF protein (lane 7). (**B**) EMSAs were performed with WT ^{32}P-labeled probe in the absence of proteins (lanes 1) or with nuclear extracts (lanes 5) isolated from Beas2B (upper panel), A549 (middle panel) and C2C12 cells (lower panel). Three or five nuclear protein complexes were detected and designated by a cell type-dependent upper-case to the left of autoradiograms. Some binding reaction mixtures included a 100-fold molar excess of the indicated cold probes (lanes 2–4). Immunologic assays were performed with either anti-SRF Ab (lanes 6), or anti-HA as irrelevant antiserum (lanes 7). As a control, the ^{32}P-labeled WT probe was incubated with anti-SRF Ab without nuclear extracts (lanes 8). In additional control experiments, radiolabeled SRE double-stranded oligonucleotide corresponding to the SRE binding site of the *c-fos* promoter was subjected to EMSAs with nuclear extracts from Beas2B cells (upper panel) in the absence (lane 9) or presence of anti-SRF antiserum (lane 10). Nuclear protein complexes that were significantly decreased or supershifted with anti-SRF Ab are indicated.

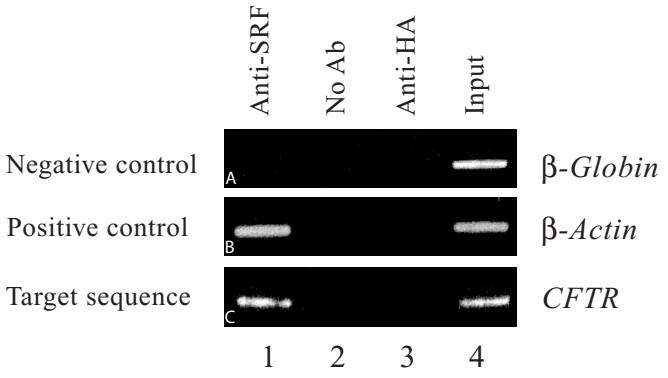

Figure 4. ChIP analysis of SRF binding to the endogenous *CFTR* minimal promoter. Chromatin immunoprecipitation was carried out as described in Materials and Methods. Sheared DNA/protein complexes were immunoprecipitated by using either an anti-SRF Ab or an irrelevant anti-HA Ab. Then, PCR was carried out to detect the endogenous CArG regions in immunoprecipitated chromatin fragments. Target promoter sequences are indicated as follow: row A, β-globin; row B, β-actin; row C, *CFTR*. Lane 1 shows amplification of target sequences in immunoprecipitated chromatin fragments with anti-SRF Ab. Lanes 2 and 3: PCR amplification of control samples, without Ab or with an irrelevant Ab. Lane 4 shows amplification of 1:100 dilution samples of total input DNA for immunoprecipitation.

isolated ChIP populations. These data show that the *CFTR*-CArG-like binding site identified within the *CFTR* minimal promoter binds SRF *in vivo*, in bronchial cell lines.

The human minimal *CFTR* promoter shows activity in both epithelial and muscular cells

As the SRF transcription factor is thought to mainly mediate the tissue-specific transcription in muscular cells, we first assessed the activity of the minimal *CFTR* promoter in both epithelial and muscular cell types. We therefore addressed the ability of the WT-pGL3 construct, previously described (12) to drive the expression in Beas2B, A549 and C2C12 cells. As shown in Figure 5A, an efficient transcription of the *CFTR* promoter could be readily observed in all three cell lines compared with monkey kidney fibroblasts (COS-7), which are negative for CFTR expression (36,37). Surprisingly, the activity of the minimal *CFTR* promoter in C2C12 cells was 4 to 5.5 times higher than that observed in Beas2B and A549 cells, respectively. Although the expression of the CFTR protein was previously evidenced in some muscle cells (57–59), it has never been investigated in mouse C2C12 myoblasts. Therefore, we investigated the CFTR expression at both mRNA and protein levels. To examine *CFTR* mRNA expression in mouse myoblasts (C2C12), total RNA isolated from epithelial and non-epithelial cells was analyzed via RT–PCR with *CFTR*-specific primers (Table 1). As shown in Figure 5B, while no PCR product for *CFTR* was seen with COS-7 cells, the expected *CFTR* amplified product was obtained for both epithelial (A549 and Beas2B) and muscular (C2C12) cell lines. No product was detected in the absence of reverse transcriptase or RNA (noted No RT or No RNA, respectively). Although the *HPRT* PCR control showed non-equivalent amounts of cDNA used in the different PCRs, densitometric analysis revealed that C2C12 cells contained an appreciable amount of *CFTR* mRNA. Further determination of CFTR expression in C2C12 myoblasts was conducted by western blot analysis (Figure 5C). Caco-2 cells were used as positive control and COS-7 as negative control. As shown in Figure 5C, while mature fully glycosylated band C CFTR was observed in A549, Beas2B and C2C12 cells, the core glycosylated band B CFTR occurred at the same molecular mass only in a subset of cell lines, indicative of potential variations in glycosylation process. To rule out the possibility of antibodies cross-reactivity or non-specific labeling, indirect immunofluorescence analysis was performed with another anti-CFTR antibody, L12B4 (Figure 5D). As expected, the Caco-2 cell line used as a positive control showed strong immunoreactivity for CFTR protein (Figure 5D, row D). In contrast, and as expected, COS-7 cells used as negative control did not stain with this anti-CFTR antibody (Figure 5D, row E). No staining was detected when the primary antibody was omitted (Figure 5D, row F). The comparison of immunofluorescence images between epithelial (Figure 5D, row A, B and *D*) and muscular (Figure 5D, row C) cells provides evidence that CFTR is significantly expressed in C2C12 myoblasts. However, because the indirect immunofluorescence experiments were performed in permeabilized cells, they do not distinguish between CFTR that is located in the apical membrane and CFTR that is located in a vesicular pool just beneath the apical membrane. These findings, together with the transcriptional activities presented above, suggest that the minimal *CFTR* promoter might contain tissue-specific enhancer(s) as well as repressive *cis*-regulatory elements that have the ability to mitigate the activity of the *CFTR* promoter between epithelial and non-epithelial lineages. Because CF affects mainly epithelial tissues and Beas2B consistently yielded higher enhancer activity than A549, we restricted subsequent studies to this bronchial epithelial cell line.

Effects of SRF on the proximal *CFTR* promoter

To assess whether SRF protein might affect *CFTR* transcriptional regulation, we took two related approaches. First, we co-transfected either exogenous full-length SRF or truncated SRF mutants with the wild-type *CFTR* minimal promoter. Second, we utilized a siRNA approach to ask whether a reduction in endogenous SRF levels could affect basal *CFTR* activation. Luciferase assays were carried out in Beas2B cells using the indicated SRF expression vectors and the WT-pGL3luciferase reporter construct (Figure 6B, left panel). The 3XSRE-fos TATA-Luciferase reporter gene was used as positive control because its transcriptional activity is highly dependent on SRF binding (Figure 6B, right panel). As expected, while this synthetic promoter containing several consensus SREs was markedly and significantly activated (>2-fold) by forced expression of full-length SRF protein (pHiv-SRF) (Figure 6B, right panel), truncated SRF mutants either containing only the amino acids 133–264 corresponding to DNA-binding domain of SRF (pHiv-DBD-SRF), or deleted of amino acids 153–165, an essential part for the DNA binding (pHiv-DN-SRF) induced modest but significant decrease of SRE activity (∼10% and ∼30%, respectively). When these SRF expression vectors were transiently co-transfected with the WT-pGL3 luciferase reporter construct, the *trans*-activator effect of SRF was notably reduced. Indeed, overexpression of full-length and dominant-negative (pHiv-DN-SRF) SRF proteins resulted in ∼50% increased and ∼30% decreased

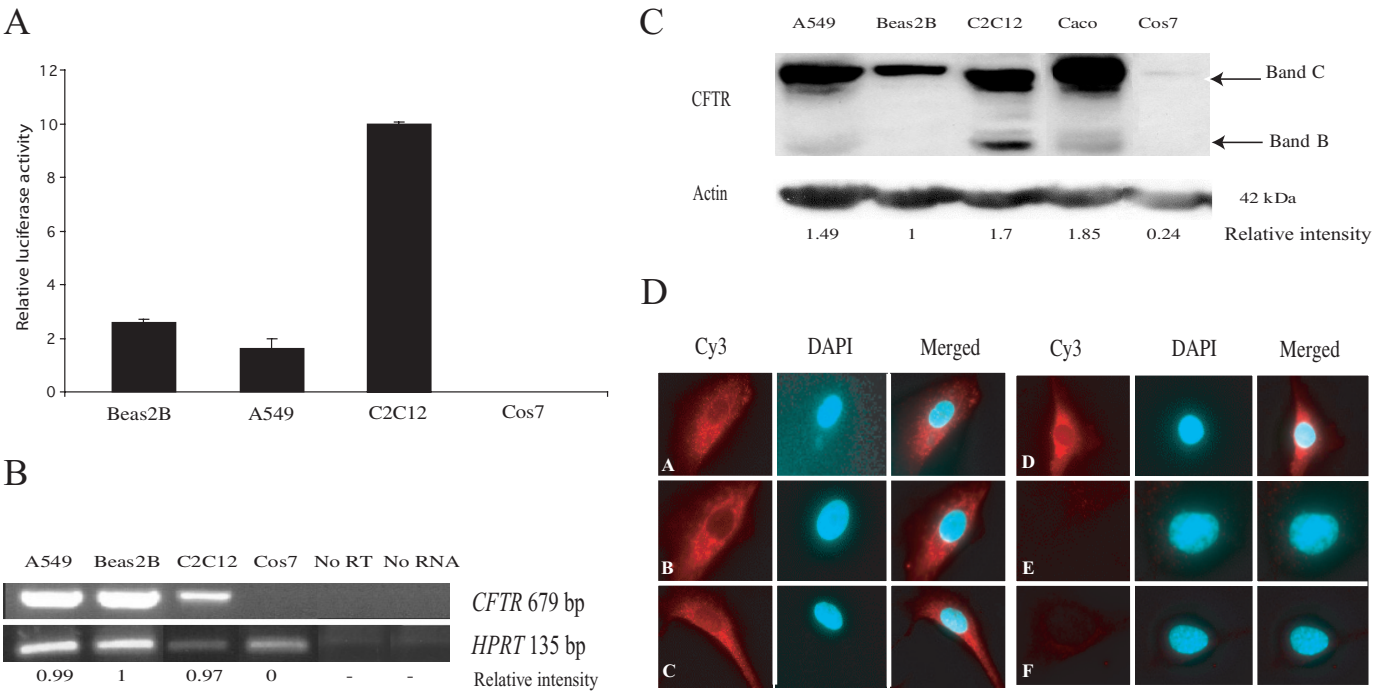

Figure 5. Analysis of *CFTR* minimal promoter activity and CFTR expression. (**A**) *CFTR* minimal promoter activities in Beas2B, A549, C2C12 and COS-7 cell lines. The amount of 1.8 μg of WT-pGL3 construct was co-transfected together with 0.2 μg of internal control pRL-SV40 containing *Renilla* luciferase. The empty pGL3-Basic vector was transfected as a negative control. Normalized luciferase values are illustrated as relative light units. The mean of two independent plasmids preps and each experiment with standard errors is shown. The experimental value for luciferase activity represented the mean ± SD of four separate experiments in triplicates. (**B**) RT–PCR analysis of *CFTR* mRNA expression. Total RNA was harvested from the indicated cell lines and subjected to PCR as described in 'Materials and Methods'. cDNA derived from COS-7 was used as a negative control. Samples without reverse transcriptase (noted No RT) or with an H_2O no-template reaction (noted No RNA) were used as additional negative controls. Samples were also amplified for *HPRT* to control for RNA degradation during DNase treatment and reverse transcription. Densitometric analysis of *CFTR* bands intensity was performed with relative *HPRT* mRNA expression in Beas2B bronchial epithelial cells. (**C**) Western blot analysis. Whole cell proteins extracts prepared from indicated cells were subjected to electrophoresis with 7% SDS–PAGE gel and transferred to supported PVDF membrane. CFTR immunoreactivity was detected using 24.1 anti-CFTR Ab as the primary antibody. Positions for the core glycosylated (band B) and mature fully glycosylated CFTR (band C) are indicated by the arrows at the right. Numbers below the β-actin panel indicate intensity values of integrated optical densities of the mature and immature CFTR bands normalized over the corresponding β-actin bands and expressed relative to the Beas2B controls bands, which are set to 1. (**D**) Indirect immunofluorescence analysis. The A549, Beas2B, C2C12, Caco-2 and COS-7 cells (rows A–E, respectively) were fixed, permeabilized, and then stained with the L12B4 anti-CFTR Ab, followed by the appropriate secondary antibody as described in 'Materials and Methods'. Left panel, cells were stained with Cy3-conjugated secondary antibody (red). Middle panel, cells were counterstained with DAPI (blue) for nuclear staining. Right panel, shown is merge of CFTR immunostaining and DAPI. Row F, Background immunofluorescence obtained in the absence of the primary antibody.

of luciferase activity, respectively (Figure 6B, left panel). Unexpectedly and inconsistent with previous study (60), the pHiv-DBD-SRF construct induced ∼40% increase of the WT-pGL3 luciferase activity. This results disparity may be explained by the fact that the c-fos promoter study (60) assessed the DBD–SRF domain activity via microinjection of corresponding truncated SRF polypeptide. Perhaps, the best explanation for this increased activity is that the DNA-binding domain of SRF, also called MADS box, is sufficient for transcriptional activation of some SRF-dependent genes because it mediates interactions with accessory co-activators (61). These results suggest that neither of the regions outside the MADS box, N- or C-terminal, appear essential for trans-activation of the *CFTR* promoter by SRF.

To further establish the role of SRF in mediating the increase in *CFTR* gene transcription, we performed siRNA experiments (Figure 6C). To demonstrate the efficacy of specific SRF siRNA construct, Beas2B cells were co-transfected with either control or SRF siRNA plasmids and western blots were performed to analyze levels of SRF in these cells. Densitometric analysis of western blot showed that endogenous SRF levels were strongly reduced in the presence of the SRF siRNA plasmid (Figure 6C, left panel). Then, control and SRF siRNA plasmids were co-transfected into Beas2B cells with either the WT-pGL3 or the 3XSRE luciferase reporter construct. As shown in Figure 6C (right panel), reduction of endogenous SRF protein level decreased the activity of both wild-type *CFTR* promoter and 3XSRE-fos TATA-Luciferase reporter constructs by ∼25%.

Taken together, these findings indicate that endogenous SRF into bronchial epithelial cells normally function as transcriptional coactivator for the CArG-mediated transactivation. However, we found that SRF activated the *CFTR* promoter less well than the SRE-containing synthetic promoter, suggesting that the CArG-like element mediated *CFTR* transcriptional activation probably required other bridging or co-activating factors.

The CArG-like element contained in the human minimal *CFTR* promoter is important but not sufficient for basal transcriptional activity in Beas2B cells

To assess the transcriptional relevance of the CArG-like binding sequence of *CFTR* minimal promoter, mutants were

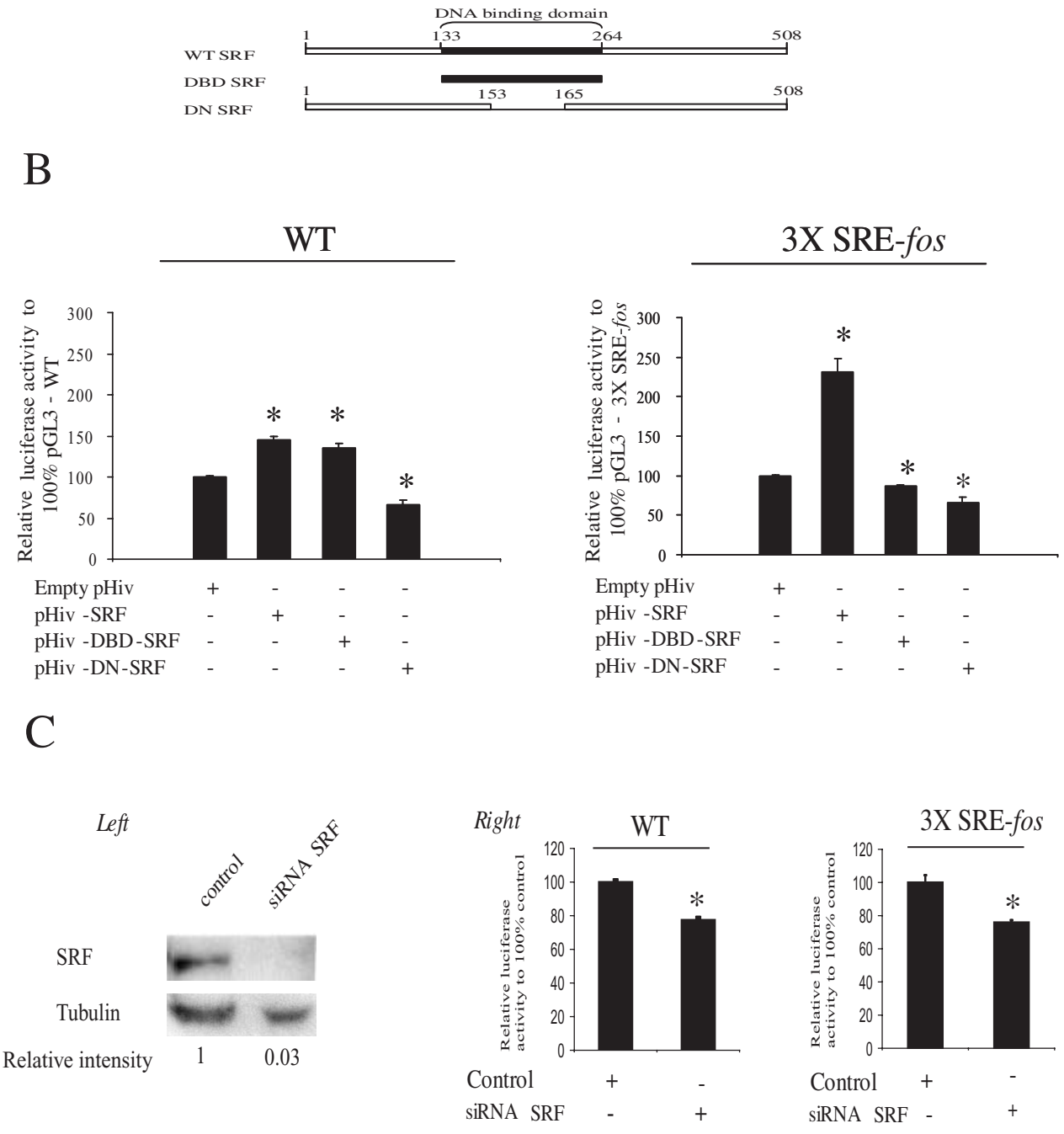

Figure 6. Effect of SRF on the activity of CArG-containing *CFTR* minimal promoter. (**A**) Schematic representation of different SRF constructs analyzed. The SRF fragments shown were cloned into the pHiv expression vector as indicated in 'Materials and Methods'. The position of the MADS box containing the DNA-binding domain and dimerization domain of SRF is depicted by black rectangle. WT SRF construct encodes a human full-length SRF open reading frame. DBD SRF construct encodes only the DNA-binding domain of SRF. DN SRF deletion construct encodes full-length SRF deleted of an essential part for the DNA binding. (**B**) Expression of exogenous SRF in Beas2B cells. Cells were co-transfected with the WT-pGL3 luciferase reporter plasmid (left panel) together with the empty pHiv vector, pHiv-SRF, pHiv-DBD-SRF or pHiv-DN-SRF constructs, as indicated below the bar diagram. As a positive control, 3XSRE luciferase reporter plasmid was used. In each experiment, a *Renilla* luciferase expression plasmid was included to normalize for transfection efficiency. For each reporter plasmid, luciferase activity (mean ± SE) is derived from 4 to 7 different transfection experiments performed in triplicate. The errors bars indicate the standard deviations. The luciferase activity value 100 was assigned to the samples co-transfected with the indicated reporter plasmid and the empty pHiv expression vector. Statistical significance is referred to differences with the activity obtained with empty expression vector. *, $P < 0.05$ versus WT or 3XSRE. (**C**) Effects of SRF siRNA on CFTR promoter activity and expression in Beas2B epithelial cells. Left panel: Beas2B cells were co-transfected with either human control siRNA vector or plasmid encoding SRF siRNA as indicated. Forty-eight hours following transfection, total proteins were harvested and analyzed by western blotting. Densitometric analysis showed a substantial decrease of endogenous SRF. Right panel: the luciferase activity value 100 was assigned to the samples co-transfected with the control siRNA. *, $P < 0.05$ versus WT or 3XSRE.

performed to create either more consensus CArG element or degenerated motif (Table 1). We used the D upper-case and the C upper-case to designate the Degenerated CArG motifs and the Consensus CArG elements, respectively. To ensure the efficacy of mutations in abrogating transcription factor binding, we first performed a series of EMSA experiments with each CArG mutant and the WT probe (Table 2). As expected, based on the sequence analysis, the mutations resulting in more degenerated CArG motifs (D1, D2, D3 and D4 mutants) completely abolished SRF-binding activity (Figure 7A, lanes 1–4), when we compared with SRF-WT complexes (Figure 7A, lane 5). In addition, the probes containing more consensus CArG boxes (C1, C2, C3, C4 and C5 mutants) bound SRF more strongly in nuclear extracts prepared from Beas2B (Figure 7A, lanes 6–10). Inclusion of an anti-SRF antibody partially abolished SRF-binding activity and resulted in a slower mobility band, confirming the identity of the binding protein (Figure 7A, lane 11). Then, minimal *CFTR* promoter constructs bearing the same consensus and disrupted CArG boxes were tested in a transient transfection assays in Beas2B cells (Figure 7B). Compared with luciferase activity resulting from the WT-pGL3 construct, variable increases in reporter activity are observed when D1, D2, D3 and D4 mutant constructs, with disrupted CArG motif, were transiently transfected. On the other hand, mutations that create more consensus CArG element result in either reducing or increasing in the transcriptional activity (Figure 7B). Consistent with the preceding gel-shift results

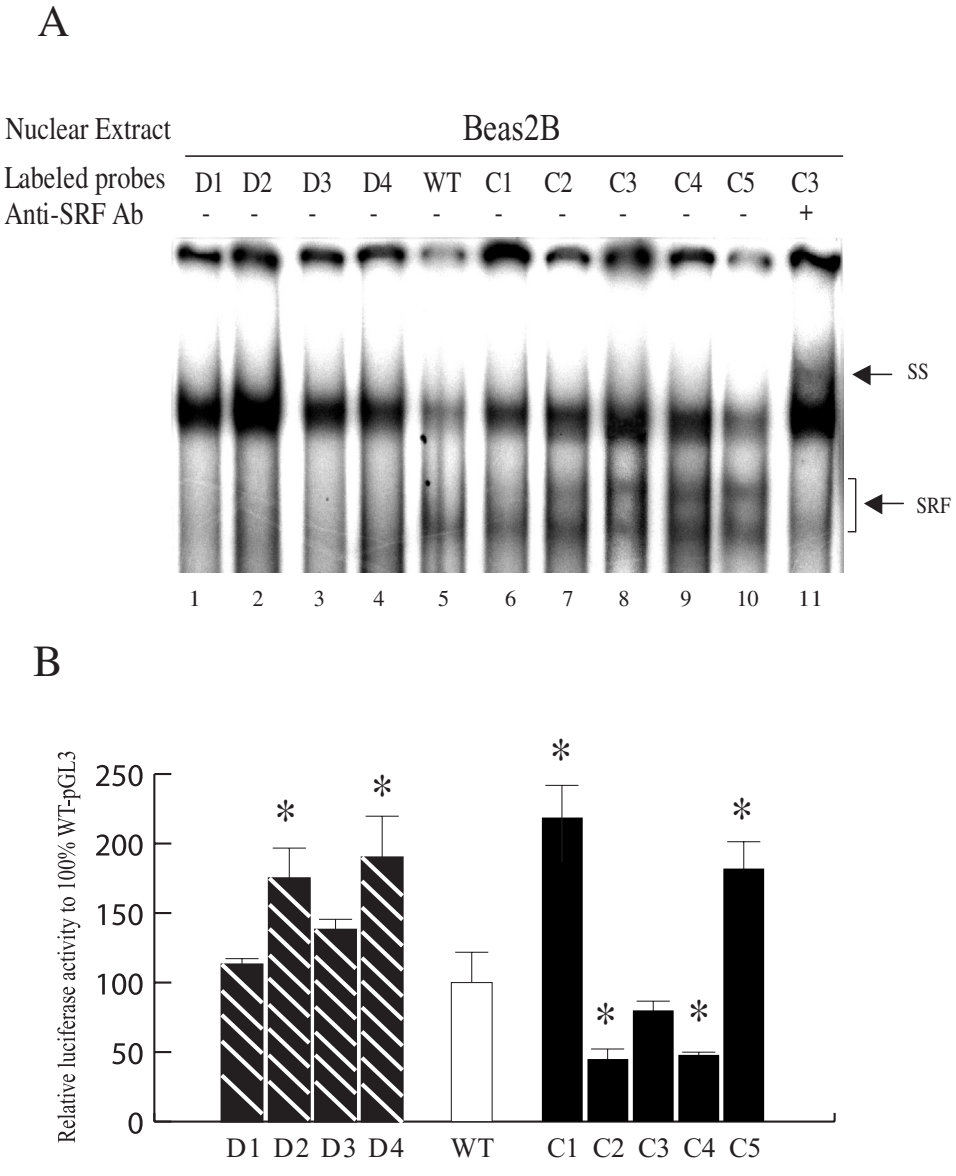

Figure 7. The CFTR-CArG-like element is not sufficient for basal transcriptional activity in Beas2B cells. (**A**) EMSA analysis with nuclear extracts from SRF protein-enriched Beas2B cells using mutated labeled oligonucleotide probes (sequences listed in Table 2). Ab against SRF was included as indicated (lane 10). The arrow SS indicates the supershifted complexes. (**B**) Basal transcriptional activity of CArG variants of the *CFTR* promoter. Luciferase activity obtained with the WT-pGL3 luciferase construct was defined as 100%, and relative luciferase activities from mutant constructs are expressed as a percentage of this value. *Firefly* luciferase activity was normalized with respect to *Renilla* luciferase activity. The errors bars indicate the standard deviations. *, $P < 0.05$ versus WT.

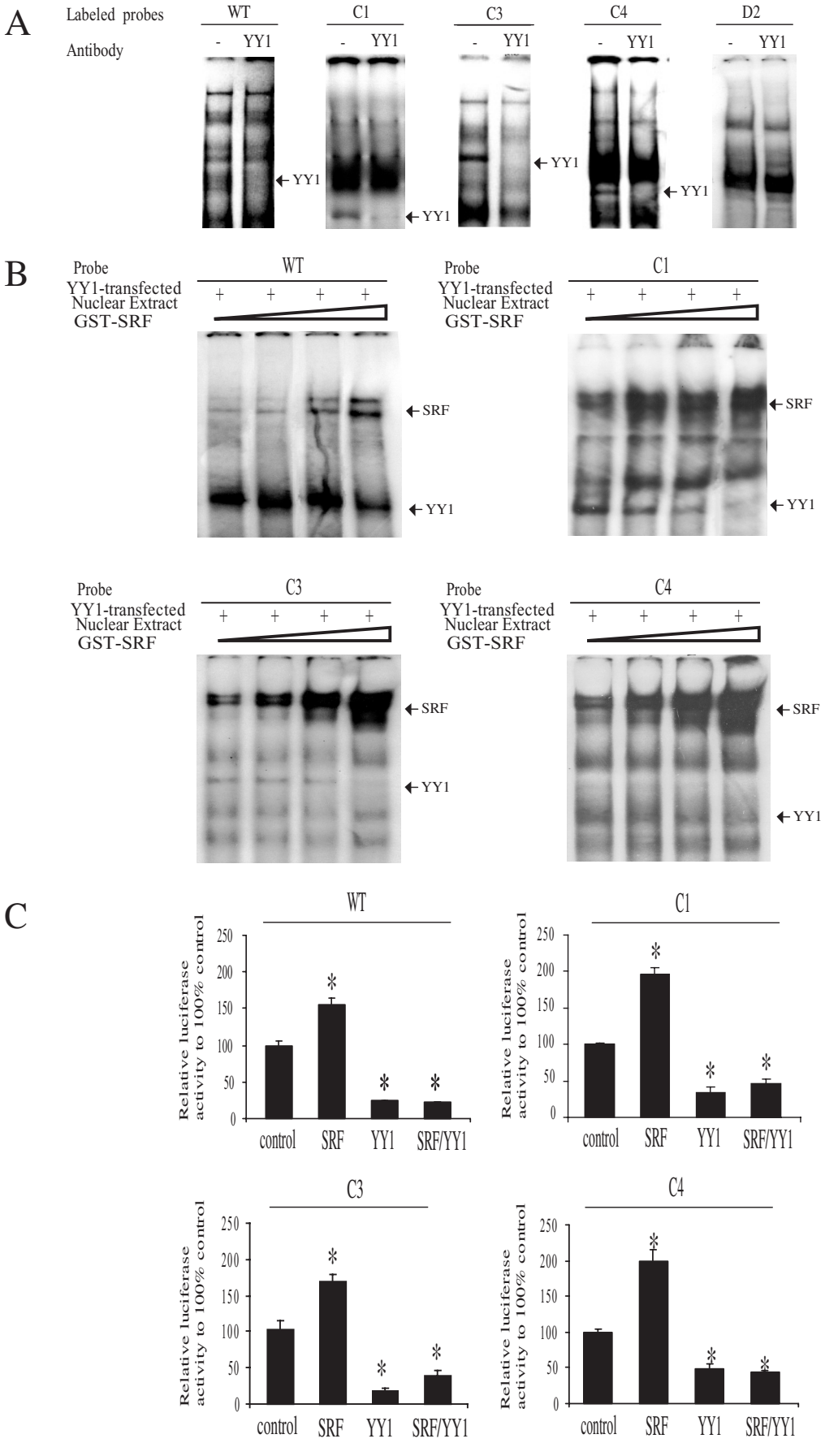

revealing an uncharacterized protein/DNA complex with slightly slower mobility and variable intensity compared with the SRF–DNA complex, these finer mutagenesis studies suggest that both co-activators and co-repressors might interact with the studied promoter sequences. Taken together, these data demonstrated that the *CFTR*-CArG-like element alone is not sufficient to confer basal transcriptional activation of the *CFTR* gene.

Functional antagonism between SRF and YY1 through competition for the *CFTR*-CArG-like binding

As a further means of establishing the role for SRF-binding CArG boxes in mediating either the *CFTR*-enhancer or silencer activity observed with the different minimal *CFTR* promoter mutants, we performed additional computational analyses. Sequence analysis of CArG boxes and their immediate flanking sequences showed that C1, C3 and C4 constructs contain consensus binding sites for a number of transcription factors, in addition to SRF, including the transcription factor YY1. These findings with previous work (12) have particularly evoked our interest to examine the role of YY1 in SRF-mediated *CFTR* transcriptional activity.

In a first set of experiments, we evaluated whether the YY1 factor contributes to the formation of nucleoprotein complexes interacting with the WT, C1, C3 and C4 radiolabeled probes. As shown in Figure 8A, incubation with specific anti-YY1 antibody resulted in either a significant decrease or total disappearance of some complexes normally formed between the CArG boxes and a component of Beas2B nuclear extracts, establishing DNA binding between YY1 and the sequences tested. As expected, control experiment performed with radiolabeled probe, D2, devoid of any YY1 binding site and the anti-YY1 antiserum did not reveal any change in electrophoretic profiles indicating specificity of the YY1 binding. Thus, these EMSAs demonstrated that the *CFTR*-CArG-like (WT probe) and more consensus CArG elements (C1 < C3 < C4) served as binding site for at least two distinct nuclear factors, namely SRF and YY1 from bronchial epithelial cells.

Then, to determine whether the interaction of these two factors with their target DNA (*CFTR*-CArG-like or more consensus CArG sequence) was either mutually inclusive or exclusive, EMSAs were conducted using bacterially expressed SRF and nuclear extracts prepared from Beas2B cells transfected with a YY1 expression vector as a source of YY1 DNA-binding activity. As shown in Figure 8B, the YY1-binding complex was significantly reduced by increasing SRF binding activity, suggesting their mutually exclusive binding to CArG sites.

Consistent with other studies (32,62), these EMSAs results suggested as a working hypothesis that both SRF and YY1 likely act as functional competitors in the *CFTR* promoter activity. Since the minimal *CFTR* promoter is activated by SRF and knowing from previous studies (30–33) that YY1 negatively regulates some promoter containing CArG elements, it seemed logical to first assess whether YY1 could also repress the *CFTR* promoter. We asked whether CArG-like-binding site in the *CFTR* promoter acted as negative regulatory elements. Several *CFTR* promoter reporter constructs containing either CArG-like (namely, WT) or consensus CArG element (C1, C3 and C4) were co-transfected with SRF and/or YY1 expression vectors into Beas2B cells. As shown in Figure 8C, while co-transfections with SRF alone resulted in 1.5- to 2-fold luciferase activation, forced expression of YY1 protein caused a strong decrease in reporter activities (~50–75% of the control luciferase value). Therefore, we wanted to determine the functional relationship of both factors in the *CFTR* activity regulation. Transient co-transfections analysis of combination of protein expression vectors showed that over-expression of SRF either did not restore (Figure 8C, panel with the WT and C4 reporter constructs) or only very slightly raised the YY1-repressed reporter activities (Figure 8C, panel with the C1 and C3 reporter constructs). These findings are consistent with results obtained from co-transfections performed with the YY1 expression vector alone and previous alpha-actin promoter studies (30–33), in which YY1 acted as a strong repressor. Taken together, these data suggested functional antagonism between SRF and YY1 through DNA-binding competition.

Identification of multiple CArG binding sites in the non-coding regions of the human *CFTR* gene and assessment of their putative functional importance

To assess the putative importance of CArG motifs in the human *CFTR* expression regulation, we performed an *in silico* inspection of additional sequences upstream of the minimal promoter and in the intronic regions. Four CArG binding sites were found in the *CFTR* promoter regions, and seven in the intronic regions. The distribution and the positions of these putative binding sites for SRF are shown in Figure 9A. Then, to confirm the computational predictions, we used several approaches. First, the nucleotide regions harboring these predicted *cis*-acting elements were analyzed for conservation in the cow, as physiologically relevant transcription factor binding sites are frequently conserved in the non-coding regions of orthologous genes (49,63). Second, the SRF-binding sites were tested by EMSAs and also for one of them by ChIP.

We showed that all the predicted CArG elements occur in highly conserved *CFTR* non-coding regions (Figure 9B), which may contain tissue-specific transcription factors (5). We provided evidence that the majority of *in silico* predicted CArG motifs form specific DNA–protein complexes with

Figure 8. Functional interplay between SRF and YY1. (**A**) YY1 binding to CFTR-CArG elements. Nuclear extracts from Beas2B cells were incubated with ^{32}P-labelled oligonucleotide probe containing either CArG-like (noted WT), consensus CArG box (noted C1, C3 and C4) in the presence or absence of specific antibody raised against YY1 as indicated. D2, which contain neither CArG element nor YY1 site, is included as negative control. Arrows indicate the position of YY1. (**B**) Mutually exclusive DNA-binding activity of YY1 versus SRF to the *CFTR*-CArG site. The same labeled CArG oligonucleotides that those used in panel A were incubated with YY1-transfected Beas2B nuclear extracts (5 μg) in the presence of increasing amounts of bacterial purified SRF (100–1000 ng). Arrows indicate the position of SRF and YY1. (**C**) Functional antagonism between SRF and YY1. Beas2B were transfected with constructs containing either the *CFTR*-CArG-like element (noted WT) or consensus *CFTR*-CArG-boxes (noted C1, C3 and C4), in the presence of SRF and/or YY1 expression vectors. Luciferase activities were normalized for transfection efficiency to the Renilla luciferase used as internal control. The luciferase activity value 100 was assigned to samples co-transfected with the indicated reporter plasmid and the empty expression vector. The mean ± SD from at least three independent experiments is represented. *, $P < 0.05$ versus WT, C1, C3 or C4.

bacterially expressed SRF protein (Figure 9C, left panel). We also demonstrated by using Beas2B nuclear extracts and supershift assays that some of these CArG elements bound *in vitro* SRF protein (Figure 9C, right panel, lanes 1, 3, 7 and 9). Finally, additional ChIP experiments indicated that the only tested CArG element, located at –2373 bp in the *CFTR* promoter, bound SRF in chromatin from intact cultured Beas2B cells (Figure 9D, lane 1). Collectively, these findings support the concept that SRF may play a key role in the *CFTR* expression regulation via binding to multiple *CFTR* CArG elements.

DISCUSSION

While great strides have been made in CFTR research with emphasis on the structure and function of this protein, only incremental advances have been achieved in the field of transcriptional regulation. In our previous works (12,20), we have identified a polymorphic CArG-like site and showed that a naturally occurring sequence variation in this motif may enhance the basal *CFTR* transcriptional activity. The goal of the present study was to better characterize the human *CFTR* promoter region encompassing the CArG-like element.

A

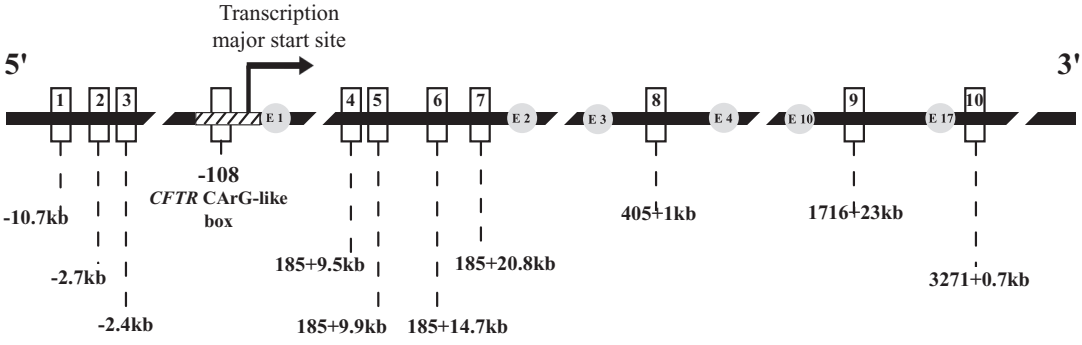

B

CArG boxes of the human *CFTR* gene and the corresponding regions of homology in the cow

CArG Number	Location of CArG in human	Human clone	Human:cow Homology	Cow clone
	Upstream exon 1			
1	-10.7 kb	AC000111 8846-9031	79%	AC089992 79372-79554
2	-2.7 kb	AC000111 16861-17034	70%	AC089992 88539-88711
3	-2.4 kb	AC000111 17241-17491	80%	AC089992 88821-89081
	Intron 1			
4	185 + 9.5 kb	AC000111 29167-29430	80%	AC089992 105768-106034
5	185 + 9.9 kb	AC000111 29699-29846	72%	AC089992 106311-106457
6	185 + 14.7 kb	AC000111 34514-34681	73%	AC089992 111573-111738
7	185 + 20.8 kb	AC000111 40563-40861	76%	AC089992 126635-126931
	Intron 3			
8	405 + 1 kb	AC000111 49422-49657	80%	AC089992 13843-14064
	Intron 10			
9	1716 + 23 kb	AC000111 122060-122341	75%	AC089993 66259-66531
	Intron 17a			
10	3271 + 0.7 kb	AC000061 1141-1494	73%	AC089993 100451-100785

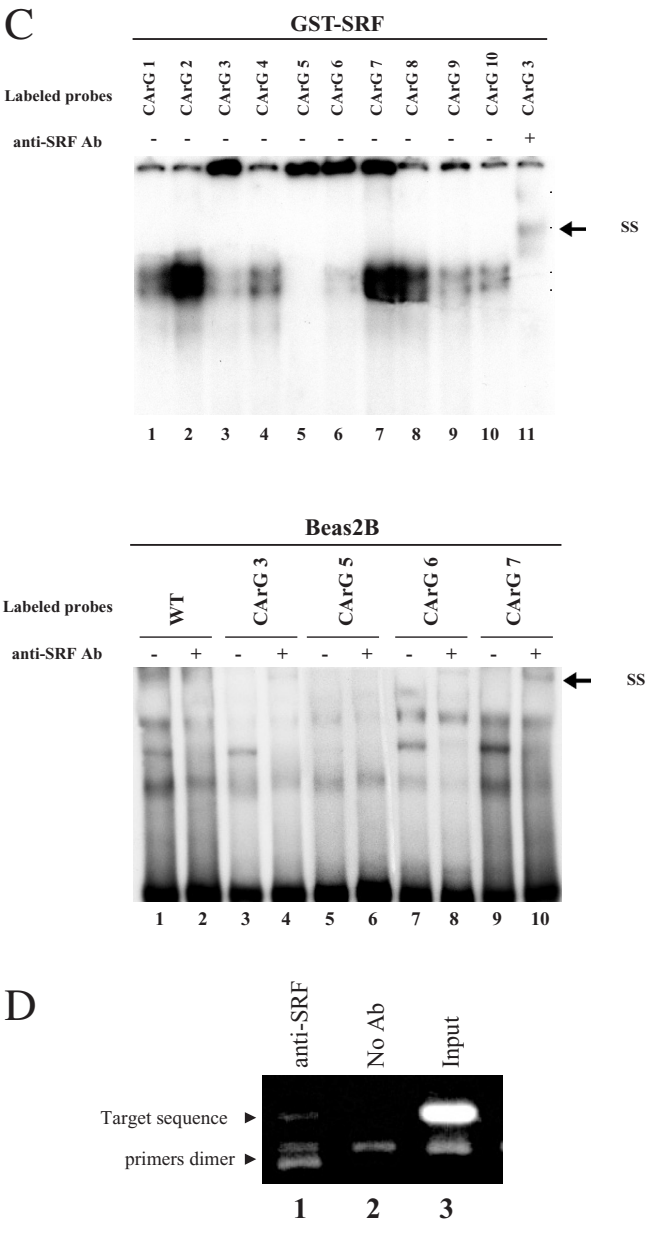

Figure 9. The *CFTR* gene untranslated regions contain multiple SRF-binding sites (CArG-boxes). (**A**) Schematic drawing of *CFTR* gene shows the exons (circles) and the location of the putative CArG boxes in the non-coding regions, including that identified in the minimal *CFTR* promoter. (**B**) The *CFTR* gene non-coding regions encompassing the putative CArG elements were analyzed for conservation in the cow. Species homology and positions of the conserved sequence within BAC clones are indicated, as reported in a recent work (49). (**C**) Comparative binding of SRF to *CFTR* CArG boxes. Each promoter and intronic CArG box-containing oligonucleotide (see Table 2) was radiolabeled and purified as described in 'Materials and Methods'. Upper panel, binding reaction was performed with bacterially expressed SRF. Ab against SRF was included as indicated. Arrow indicates specific DNA–SRF complexes and SS indicates the Ab-supershifted complexes. Lower panel, EMSA analysis with nuclear extracts from Beas2B cells using mutated labeled oligonucleotide probes. (**D**) ChIP analysis of SRF binding to the endogenous CArG regions. Lane 1 shows amplification of target sequence in immunoprecipitated chromatin fragments with anti-SRF Ab. The target sequence encompasses a CArG element, located to –2373 bp in the minimal *CFTR* promoter. Lane 2 shows PCR amplification of a control sample, without Ab. Lane 3 shows amplification of 1:100 dilution samples of total input DNA for immunoprecipitation.

Comparisons of nucleotide sequences of this *CFTR* promoter region in eight mammalian species representing three different orders (Primates, Artiodactyla and Lagomorpha) revealed high levels of conservation of the minimal promoter region, as described previously (64). However, the CArG-like element (***G***C(T/A)$_6$GG), which does not conform to the authentic CArG box (CC(T/A)$_6$GG), is absent from three species (sheep, cow and rabbit). Even though this motif occurs in only a subset of the input sequences, it does not necessarily mean that it is of no functional importance. Instances of *cis*-regulatory elements being species-specific have been already reported for the *CFTR* gene (50). More generally, it is well known that some transcription factors can tolerate more than one type of nucleotide at a given position of the binding site. Instances of substitutions in both the central core of the CArG element and the highly conserved contact points for SRF, at the terminal ends, not impairing SRF binding have been previously reported (48,65–68). Taken together, these data support the notion that the *CFTR*-CArG-like element has possible important implication in the *CFTR* transcriptional regulation.

Interestingly, analysis of SRF expression has revealed relatively high expression levels of SRF protein in the bronchial epithelial cells (Figure 2), as shown in other differentiated epithelial cells (27). Accumulating evidence supports the concept that SRF could contribute to the *CFTR* expression regulation. In addition to regulating growth-responsive genes and numerous muscle-specific genes (22,69), SRF is also described as a key *trans*-binding factor in various important physiological events. For example, SRF has been shown to regulate pulmonary development in Drosophila (28), to promote both re-epithelialization and muscular structure restoration during gastric ulcer healing (70) and more recently to be involved in the regulation of endoplasmic reticulum-targeted gene (67). Therefore, it was relevant to examine the potential role of SRF on the *CFTR* transcriptional activity.

In the present study, we demonstrated that *CFTR*-CArG-like element forms specific DNA–protein complexes that include SRF protein as part of the complex, *in vitro* and *in vivo* (Figures 3 and 4). We have investigated the expression driven by the proximal human *CFTR* promoter in a pGL3 construct in both epithelial and myoblasts lines. Results of our transient transfections of 3XSRE-fos TATA and WT-pGL3 luciferase reporter genes showed that the human minimal *CFTR* promoter encompassing a CArG-like motif was sufficient to drive the expression in both cell types (Figure 5). Consistent with other studies showing *CFTR* expression in smooth muscle tissue (71,72), our results demonstrated that the human *CFTR* minimal promoter had the ability to drive the expression in muscle lineages. Our transient co-transfections analyses performed with full-length and dominant-negative SRF forms expression vectors, and also specific SRF siRNA constructs (Figure 6, panels B and C) provide the first evidence for a positive role of the SRF protein in the regulation of the human *CFTR* promoter. However, the SRF-induced *CFTR* transactivation, though significant, is relatively modest. These data with the results of finer mutagenesis studies presented in Figure 7 support the concept that SRF alone is not sufficient to drive the basal expression of the *CFTR* gene. As suggested by other previous studies (73–75), it is likely that additional factors might be required to optimally drive

the *CFTR* promoter, as well as to specify the cell-type-restricted expression. Since YY1 was previously shown to bind the *CFTR* promoter (12) and a subset of SREs serve as binding sites for YY1 (30–33), we first evaluated this candidate in the SRF-mediated *CFTR* transcriptional activity. The data analysis suggests a functional antagonism between SRF and YY1 through binding competition for the *CFTR*-CArG-like box. However, the analysis of combinatorial co-transfection studies, presented in Figure 8C, suggests that the functional interplay between SRF and YY1, alone, is not sufficient to account for basal *CFTR* transcriptional activation. Further studies will be necessary to determine whether another player might be involved in this functional interplay and accounted for the basal transcriptional *CFTR* activity observed in the Beas2B bronchial epithelial cells.

Interestingly, we showed that, in addition to the CArG-like element defined in the minimal promoter of the *CFTR* gene, there are three CArG motifs located at the 5′ end of the gene and seven are present in the intronic regions (Figure 9). We also evidenced SRF binding to CArG elements of the endogenous *CFTR* gene in the context of intact chromatin (Figures 4 and 9D). Although the role of these more distal CArG boxes has yet to be assessed, these findings are of major importance, since it has been shown that optimal activity of the SRF-dependent target genes may require a number of CArG boxes, including those that are defined in the intronic region (66,67,76). Moreover, as already suggested for the α-actin promoters (32,74), perhaps the presence multiple CArG elements in the *CFTR* gene with cooperative binding events might be essential for SRF to prevent YY1 from binding to the *CFTR* promoter. Clearly, further studies are needed to directly investigate the role of these multiple CArG elements in transcriptional regulation of the *CFTR* gene.

Taken together, our results demonstrated for the first time that the human *CFTR* promoter is a novel SRF target gene, subject to modest but significant SRF activation partially due to functional antagonism between YY1 and SRF through mutually exclusive DNA-binding activities of YY1 versus SRF to the *CFTR*-CArG-like site.

A critical question is, thus, how might SRF contribute to orchestrating cell-restricted and context-dependent programs of *CFTR* gene expression? Our findings and investigations to date clearly indicate the presence of several different underlying mechanisms of SRF-dependent transcriptional activation, as represented in Figure 10. These might include association of SRF with a variety of cell-restricted co-factors (noted in gray bubbles, Figure 10), such as MRTF-A highly expressed in epithelial cells of the lung, kidney, colon and testis, and MRTF-B also expressed in smooth muscle cells (77), ternary complex factors, such as p62 and SAP-1 (25,78) and remodeling chromatin co-factors in an HAT-dependent manner, such as the CREB-binding protein (79). In addition, it is well known that binding of SRF to the CArG box induces an acute bend in the DNA and that this bending may vary with changing base compositions across the CArG box (80). Such bending can probably facilitate interactions with other proteins already involved in the *CFTR* expression regulation, such as NF-κB (13) and C/EBP (9) and described as interacting with SRF (81). Finally, the Ras-related GTPases family (rac, RhoA and cdc42) might have a critical role in the activation of SRF (82). Indeed, it is reported that

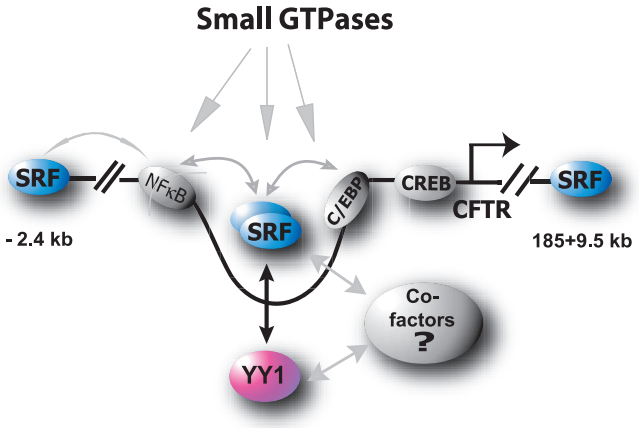

Figure 10. Schematic model depicting potential mechanism that might contribute to epithelial-specific regulation of the *CFTR* gene. In this model, arrows and bubbles marked in gray indicate multiple potential SRF-mediated regulation pathways, such as protein–protein interaction and potential induction by the Ras-related GTPases cascades. Blue and pink bubbles indicate *trans*-factors identified in this study that contribute to the basal CFTR transcriptional activity. Black and double arrow shows the functional antagonism between YY1 and SRF identified in this study through the CFTR-CArG-like element characterization.

RhoA-induced SRF activation occurs through a phenomenon of 'actin treadmilling' restricted to CArG-dependent genes that do not have adjacent ETS-binding sites (e.g. smooth muscle cell restricted CArG genes) (83,84). Moreover, it has been shown that the activation of SRF may be mediated by the NF-κB and C/EBP transcription factors (81).

These data provide the foundation for further studies on the regulation of *CFTR* and will unable the rational design of further functional studies, including various strategies aiming to further dissect the different regulation pathways.

ACKNOWLEDGEMENTS

This study was supported by grants from both French associations: Vaincre La Mucoviscidose (VLM) and Fondation pour la Recherche Medicale (FRM). J.D. was supported by PhD fellowship grants from the VLM. We are particularly indebted to A. Fernandez and N. Lamb for their continuous support to A.L. and for critical reading of the manuscript and. The authors thank G. Carnac for many valuable discussions and suggestions. The authors also thank the investigators mentioned in Materials and Methods for the kind gifts of crucial reagents. Funding to pay the Open Access publication charges for this article was provided by the Centre National de la Recherche Scientifique (CNRS).

Conflict of interest statement. None declared.

REFERENCES

1. Crawford,I., Maloney,P.C., Zeitlin,P.L., Guggino,W.B., Hyde,S.C., Turley,H., Gatter,K.C., Harris,A. and Higgins,C.F. (1991) Immunocytochemical localization of the cystic fibrosis gene product CFTR. *Proc. Natl Acad. Sci. USA*, **88**, 9262–9266.
2. Denning,G.M., Ostedgaard,L.S., Cheng,S.H., Smith,A.E. and Welsh,M.J. (1992) Localization of cystic fibrosis transmembrane conductance regulator in chloride secretory epithelia. *J. Clin. Invest.*, **89**, 339–349.

3. Engelhardt,J.F., Yankaskas,J.R., Ernst,S.A., Yang,Y., Marino,C.R., Boucher,R.C., Cohn,J.A. and Wilson,J.M. (1992) Submucosal glands are the predominant site of CFTR expression in the human bronchus. *Nature Genet*., **2**, 240–248.
4. Trezise,A.E., Linder,C.C., Grieger,D., Thompson,E.W., Meunier,H., Griswold,M.D. and Buchwald,M. (1993) CFTR expression is regulated during both the cycle of the seminiferous epithelium and the oestrous cycle of rodents. *Nature Genet*., **3**, 157–164.
5. Mouchel,N., Broackes-Carter,F. and Harris,A. (2003) Alternative 5′ exons of the CFTR gene show developmental regulation. *Hum. Mol. Genet*., **12**, 759–769.
6. Yoshimura,K., Nakamura,H., Trapnell,B.C., Dalemans,W., Pavirani,A., Lecocq,J.P. and Crystal,R.G. (1991) The cystic fibrosis gene has a 'housekeeping'-type promoter and is expressed at low levels in cells of epithelial origin. *J. Biol. Chem*., **266**, 9140–9144.
7. Koh,J., Sferra,T.J. and Collins,F.S. (1993) Characterization of the cystic fibrosis transmembrane conductance regulator promoter region. Chromatin context and tissue-specificity. *J. Biol. Chem*., **268**, 15912–15921.
8. White,N.L., Higgins,C.F. and Trezise,A.E. (1998) Tissue-specific *in vivo* transcription start sites of the human and murine cystic fibrosis genes. *Hum. Mol. Genet*., **7**, 363–369.
9. Pittman,N., Shue,G., LeLeiko,N.S. and Walsh,M.J. (1995) Transcription of cystic fibrosis transmembrane conductance regulator requires a CCAAT-like element for both basal and cAMP-mediated regulation. *J. Biol. Chem*., **270**, 28848–28857.
10. Matthews,R.P. and McKnight,G.S. (1996) Characterization of the cAMP response element of the cystic fibrosis transmembrane conductance regulator gene promoter. *J. Biol. Chem*., **271**, 31869–31877.
11. McDonald,R.A., Matthews,R.P., Idzerda,R.L. and McKnight,G.S. (1995) Basal expression of the cystic fibrosis transmembrane conductance regulator gene is dependent on protein kinase A activity. *Proc. Natl Acad. Sci. USA*, **92**, 7560–7564.
12. Romey,M.C., Pallares-Ruiz,N., Mange,A., Mettling,C., Peytavi,R., Demaille,J. and Claustres,M. (2000) A naturally occurring sequence variation that creates a YY1 element is associated with increased cystic fibrosis transmembrane conductance regulator gene expression. *J. Biol. Chem*., **275**, 3561–3567.
13. Brouillard,F., Bouthier,M., Leclerc,T., Clement,A., Baudouin-Legros,M. and Edelman,A. (2001) NF-kappa B mediates up-regulation of CFTR gene expression in Calu-3 cells by interleukin-1beta. *J. Biol. Chem*., **276**, 9486–9491.
14. Li,S., Moy,L., Pittman,N., Shue,G., Aufiero,B., Neufeld,E.J., LeLeiko,N.S. and Walsh,M.J. (1999) Transcriptional repression of the cystic fibrosis transmembrane conductance regulator gene, mediated by CCAAT displacement protein/cut homolog, is associated with histone deacetylation. *J. Biol. Chem*., **274**, 7803–7815.
15. Smith,A.N., Barth,M.L., McDowell,T.L., Moulin,D.S., Nuthall,H.N., Hollingsworth,M.A. and Harris,A. (1996) A regulatory element in intron 1 of the cystic fibrosis transmembrane conductance regulator gene. *J. Biol. Chem*., **271**, 9947–9954.
16. Smith,D.J., Nuthall,H.N., Majetti,M.E. and Harris,A. (2000) Multiple potential intragenic regulatory elements in the CFTR gene. *Genomics*, **64**, 90–96.
17. Rowntree,R.K., Vassaux,G., McDowell,T.L., Howe,S., McGuigan,A., Phylactides,M., Huxley,C. and Harris,A. (2001) An element in intron 1 of the CFTR gene augments intestinal expression *in vivo*. *Hum. Mol. Genet*., **10**, 1455–1464.
18. Phylactides,M., Rowntree,R., Nuthall,H., Ussery,D., Wheeler,A. and Harris,A. (2002) Evaluation of potential regulatory elements identified as DNase I hypersensitive sites in the CFTR gene. *Eur. J. Biochem*., **269**, 553–559.
19. Mouchel,N., Henstra,S.A., McCarthy,V.A., Williams,S.H., Phylactides,M. and Harris,A. (2004) HNF1alpha is involved in tissue-specific regulation of CFTR gene expression. *Biochem. J*., **378**, 909–918.
20. Romey,M.C., Guittard,C., Chazalette,J.P., Frossard,P., Dawson,K.P., Patton,M.A., Casals,T., Bazarbachi,T., Girodon,E., Rault,G. *et al*. (1999) Complex allele [−102T>A+S549R(T>G)] is associated with milder forms of cystic fibrosis than allele S549R(T>G) alone. *Hum. Genet*., **105**, 145–150.
21. Treisman,R. (1986) Identification of a protein-binding site that mediates transcriptional response of the c-fos gene to serum factors. *Cell*, **46**, 567–574.
22. Miano,J.M. (2003) Serum response factor: toggling between disparate programs of gene expression. *J. Mol. Cell Cardiol*., **35**, 577–593.
23. Shore,P. and Sharrocks,A.D. (1995) The MADS-box family of transcription factors. *Eur. J. Biochem*., **229**, 1–13.
24. Browning,C.L., Culberson,D.E., Aragon,I.V., Fillmore,R.A., Croissant,J.D., Schwartz,R.J. and Zimmer,W.E. (1998) The developmentally regulated expression of serum response factor plays a key role in the control of smooth muscle-specific genes. *Dev. Biol*., **194**, 18–37.
25. Camoretti-Mercado,B., Dulin,N.O. and Solway,J. (2003) Serum response factor function and dysfunction in smooth muscle. *Respir. Physiol. Neurobiol*., **137**, 223–235.
26. Magnaghi-Jaulin,L., Masutani,H., Lipinski,M. and Harel-Bellan,A. (1996) Analysis of SRF, SAP-1 and ELK-1 transcripts and proteins in human cell lines. *FEBS Lett*., **391**, 247–251.
27. Chai,J., Baatar,D., Moon,W. and Tarnawski,A. (2002) Expression of serum response factor in normal rat gastric mucosa. *J. Physiol. Pharmacol*., **53**, 289–294.
28. Guillemin,K., Groppe,J., Ducker,K., Treisman,R., Hafen,E., Affolter,M. and Krasnow,M.A. (1996) The pruned gene encodes the Drosophila serum response factor and regulates cytoplasmic outgrowth during terminal branching of the tracheal system. *Development*, **122**, 1353–1362.
29. Yang,Y., Zhe,X., Phan,S.H., Ullenbruch,M. and Schuger,L. (2003) Involvement of serum response factor isoforms in myofibroblast differentiation during bleomycin-induced lung injury. *Am. J. Respir. Cell Mol. Biol*., **29**, 583–590.
30. Liu,T., Wu,J. and He,F. (2000) Evolution of *cis*-acting elements in 5′ flanking regions of vertebrate actin genes. *J. Mol. Evol*., **50**, 22–30.
31. Natesan,S. and Gilman,M. (1995) YY1 facilitates the association of serum response factor with the c-fos serum response element. *Mol. Cell. Biol*, **15**, 5975–5982.
32. Chen,C.Y. and Schwartz,R.J. (1997) Competition between negative acting YY1 versus positive acting serum response factor and tinman homologue Nkx-2.5 regulates cardiac alpha-actin promoter activity. *Mol. Endocrinol*., **11**, 812–822.
33. Martin,K.A., Gualberto,A., Colman,M.F., Lowry,J. and Walsh,K. (1997) A competitive mechanism of CArG element regulation by YY1 and SRF: implications for assessment of Phox1/MHox transcription factor interactions at CArG elements. *DNA Cell Biol*, **16**, 653–661.
34. Mohamed,A., Ferguson,D., Seibert,F.S., Cai,H.M., Kartner,N., Grinstein,S., Riordan,J.R. and Lukacs,G.L. (1997) Functional expression and apical localization of the cystic fibrosis transmembrane conductance regulator in MDCK I cells. *Biochem. J*, **322**, 259–265.
35. Bradbury,N.A., Clark,J.A., Watkins,S.C., Widnell,C.C. and Smith,H.S. (1999) Characterization of the internalization pathways for the cystic fibrosis transmembrane conductance regulator. *Am. J. Physiol*., **276**, L659–L668.
36. Tousson,A., Van Tine,B.A., Naren,A.P., Shaw,G.M. and Schwiebert,L.M. (1998) Characterization of CFTR expression and chloride channel activity in human endothelia. *Am. J. Physiol*, **275**, C1555–C1564.
37. Peter,K., Varga,K., Bebok,Z., McNicholas-Bevensee,C.M., Schwiebert,L., Sorscher,E.J., Schwiebert,E.M. and Collawn,J.F. (2002) Ablation of internalization signals in the carboxyl-terminal tail of the cystic fibrosis transmembrane conductance regulator enhances cell surface expression. *J. Biol. Chem*., **277**, 49952–49957.
38. Chou,J.L., Rozmahel,R. and Tsui,L.C. (1991) Characterization of the promoter region of the cystic fibrosis transmembrane conductance regulator gene. *J. Biol. Chem*., **266**, 24471–24476.
39. Cheng,S.H., Fang,S.L., Zabner,J., Marshall,J., Piraino,S., Schiavi,S.C., Jefferson,D.M., Welsh,M.J. and Smith,A.E. (1995) Functional activation of the cystic fibrosis trafficking mutant delta F508-CFTR by overexpression. *Am. J. Physiol*, **268**, L615–L624.
40. Shore,P. and Sharrocks,A.D. (1994) The transcription factors Elk-1 and serum response factor interact by direct protein-protein contacts mediated by a short region of Elk-1. *Mol. Cell. Biol*., **14**, 3283–3291.
41. Romey,M.C., Tuffery,S., Desgeorges,M., Bienvenu,T., Demaille,J. and Claustres,M. (1996) Transcript analysis of CFTR frameshift mutations in lymphocytes using the reverse transcription-polymerase chain reaction technique and the protein truncation test. *Hum. Genet*., **98**, 328–332.
42. Kartner,N., Augustinas,O., Jensen,T.J., Naismith,A.L. and Riordan,J.R. (1992) Mislocalization of delta F508 CFTR in cystic fibrosis sweat gland. *Nature Genet*., **1**, 321–327.

43. Mendes,F., Farinha,C.M., Roxo-Rosa,M., Fanen,P., Edelman,A., Dormer,R., McPherson,M., Davidson,H., Puchelle,E., De Jonge,H. *et al.* (2004) Antibodies for CFTR studies. *J. Cyst. Fibros.* (Suppl. 2), 69–72.
44. Farinha,C.M., Mendes,F., Roxo-Rosa,M., Penque,D. and Amaral,M.D. (2004) A comparison of 14 antibodies for the biochemical detection of the cystic fibrosis transmembrane conductance regulator protein. *Mol. Cell. Probes*, **18**, 235–242.
45. Thompson,J.D., Higgins,D.G. and Gibson,T.J. (1994) CLUSTAL W: improving the sensitivity of progressive multiple sequence alignment through sequence weighting, positions-specific gap penalties and weight matrix choice. *Nucleic Acids Res.*, **22**, 4673–4680.
46. Romey,M.C., Guittard,C., Carles,S., Demaille,J., Claustres,M. and Ramsay,M. (1999) First putative sequence alterations in the minimal CFTR promoter region. *J. Med. Genet.*, **36**, 263–264.
47. Herschman,H.R. (1991) Primary response genes induced by growth factors and tumor promoters. *Annu. Rev. Biochem.*, **60**, 281–319.
48. Hirschi,K.K., Lai,L., Belaguli,N.S., Dean,D.A., Schwartz,R.J. and Zimmer,W.E. (2002) Transforming growth factor-beta induction of smooth muscle cell phenotype requires transcriptional and post-transcriptional control of serum response factor. *J. Biol. Chem.*, **277**, 6287–6295.
49. Williams,S.H., Sahota,V., Palmai-Pallag,T., Tebbutt,S.J., Walker,J. and Harris,A. (2003) Evaluation of gene targeting by homologous recombination in ovine somatic cells. *Mol. Reprod. Dev.*, **66**, 115–125.
50. Vuillaumier,S., Dixmeras,I., Messai,H., Lapoumeroulie,C., Lallemand,D., Gekas,J., Chehab,F.F., Perret,C., Elion,J. and Denamur,E. (1997) Cross-species characterization of the promoter region of the cystic fibrosis transmembrane conductance regulator gene reveals multiple levels of regulation. *Biochem. J.*, **327**, 651–662.
51. Williams,S.H., Mouchel,N. and Harris,A. (2003) A comparative genomic analysis of the cow, pig, and human CFTR genes identifies potential intronic regulatory elements. *Genomics*, **81**, 628–639.
52. Davis,F.J., Gupta,M., Pogwizd,S.M., Bacha,E., Jeevanandam,V. and Gupta,M.P. (2002) Increased expression of alternatively spliced dominant-negative isoform of SRF in human failing hearts. *Am. J. Physiol. Heart. Circ. Physiol.*, **282**, H1521–H1533.
53. Psichari,E., Balmain,A., Plows,D., Zoumpourlis,V. and Pintzas,A. (2002) High activity of serum response factor in the mesenchymal transition of epithelial tumor cells is regulated by RhoA signaling. *J. Biol. Chem.*, **277**, 29490–29495.
54. Spencer,J.A. and Misra,R.P. (1996) Expression of the serum response factor gene is regulated by serum response factor binding sites. *J. Biol. Chem.*, **271**, 16535–16543.
55. Treisman,R. (1992) The serum response element. *Trends. Biochem. Sci.*, **17**, 423–426.
56. Gualberto,A., LePage,D., Pons,G., Mader,S.L., Park,K., Atchison,M.L. and Walsh,K. (1992) Functional antagonism between YY1 and the serum response factor. *Mol. Cell. Biol.*, **12**, 4209–4214.
57. Gadsby,D.C., Nagel,G. and Hwang,T.C. (1995) The CFTR chloride channel of mammalian heart. *Annu. Rev. Physiol.*, **57**, 387–416.
58. Tilly,B.C., Bezstarosti,K., Boomaars,W.E., Marino,C.R., Lamers,J.M. and de Jonge,H.R. (1996) Expression and regulation of chloride channels in neonatal rat cardiomyocytes. *Mol. Cell. Biochem*, **157**, 129–135.
59. Robert,R., Thoreau,V., Norez,C., Cantereau,A., Kitzis,A., Mettey,Y., Rogier,C. and Becq,F. (2004) Regulation of the cystic fibrosis transmembrane conductance regulator channel by beta-adrenergic agonists and vasoactive intestinal peptide in rat smooth muscle cells and its role in vasorelaxation. *J. Biol. Chem*, **279**, 21160–21168.
60. Gauthier-Rouviere,C., Cai,Q.Q., Lautredou,N., Fernandez,A., Blanchard,J.M. and Lamb,N.J. (1993) Expression and purification of the DNA-binding domain of SRF: SRF-DB, a part of a DNA-binding protein which can act as a dominant negative mutant *in vivo*. *Exp. Cell. Res.*, **209**, 208–215.
61. Hill,C.S., Wynne,J. and Treisman,R. (1994) Serum-regulated transcription by serum response factor (SRF): a novel role for the DNA binding domain. *EMBO J.*, **13**, 5421–5432.
62. Ellis,P.D., Martin,K.M., Rickman,C., Metcalfe,J.C. and Kemp,P.R. (2002) Increased actin polymerization reduces the inhibition of serum response factor activity by Yin Yang 1. *Biochem. J*, **364**, 547–554.
63. Wasserman,W.W., Palumbo,M., Thompson,W., Fickett,J.W. and Lawrence,C.E. (2000) Human-mouse genome comparisons to locate regulatory sites. *Nature Genet.*, **26**, 225–228.
64. Denamur,E. and Chehab,F.F. (1994) Analysis of the mouse and rat CFTR promoter regions. *Hum. Mol. Genet.*, **3**, 1089–1094.
65. Zilberman,A., Dave,V., Miano,J., Olson,E.N. and Periasamy,M. (1998) Evolutionarily conserved promoter region containing CArG*-like elements is crucial for smooth muscle myosin heavy chain gene expression. *Circ. Res.*, **82**, 566–575.
66. Miano,J.M., Carlson,M.J., Spencer,J.A. and Misra,R.P. (2000) Serum response factor-dependent regulation of the smooth muscle calponin gene. *J. Biol. Chem.*, **275**, 9814–9822.
67. Streb,J.W. and Miano,J.M. (2005) AKAP12alpha, an atypical serum response factor-dependent target gene. *J. Biol. Chem.*, **280**, 4125–4134.
68. L'Honore,A., Lamb,N.J., Vandromme,M., Turowski,P., Carnac,G. and Fernandez,A. (2003) MyoD distal regulatory region contains an SRF binding CArG element required for MyoD expression in skeletal myoblasts and during muscle regeneration. *Mol. Biol. Cell*, **14**, 2151–2162.
69. Treisman,R. (1995) Journey to the surface of the cell: Fos regulation and the SRE. *EMBO J.*, **14**, 4905–4913.
70. Chai,J., Baatar,D. and Tarnawski,A. (2004) Serum response factor promotes re-pithelialization and muscular structure restoration during gastric ulcer healing. *Gastroenterology*, **126**, 1809–1818.
71. Robert,R., Thoreau,V., Norez,C., Cantereau,A., Kitzis,A., Mettey,Y., Rogier,C. and Becq,F. (2004) Regulation of the cystic fibrosis transmembrane conductance regulator channel by beta-adrenergic-agonists and VIP in rat smooth muscle cells and its role in vasorelaxation. *J. Biol. Chem*, **279**, 21160–21168.
72. Davies,W.L., Vandenberg,J.I., Sayeed,R.A. and Trezise,A.E. (2004) Cardiac expression of the cystic fibrosis transmembrane conductance regulator involves novel exon 1 usage to produce an unique amino-terminal protein. *J. Biol. Chem.*, **279**, 15877–15887.
73. Chow,K.L. and Schwartz,R.J. (1990) A combination of closely associated positive and negative *cis*-acting promoter elements regulates transcription of the skeletal alpha-actin gene. *Mol. Cell. Biol.*, **10**, 528–538.
74. Lee,T.C., Chow,K.L., Fang,P. and Schwartz,R.J. (1991) Activation of skeletal alpha-actin gene transcription: the cooperative formation of serum response factor-binding complexes over positive *cis*-acting promoter serum response elements displaces a negative-acting nuclear factor enriched in replicating myoblasts and nonmyogenic cells. *Mol. Cell. Biol.*, **11**, 5090–5100.
75. Moss,J.B., McQuinn,T.C. and Schwartz,R.J. (1994) The avian cardiac alpha-actin promoter is regulated through a pair of complex elements composed of E boxes and serum response elements that bind both positive- and negative-acting factors. *J. Biol. Chem*, **269**, 12731–12740.
76. Mack,C.P. and Owens,G.K. (1999) Regulation of smooth muscle alpha-actin expression *in vivo* is dependent on CArG elements within the 5′ and first intron promoter regions. *Circ. Res.*, **84**, 852–861.
77. Wang,D.Z., Li,S., Hockemeyer,D., Sutherland,L., Wang,Z., Schratt,G., Richardson,J.A., Nordheim,A. and Olson,E.N. (2002) Potentiation of serum response factor activity by a family of myocardin-related transcription factors. *Proc. Natl Acad. Sci. USA*, **99**, 14855–14860.
78. Mo,Y., Ho,W., Johnston,K. and Marmorstein,R. (2001) Crystal structure of a ternary SAP-1/SRF/c-fos SRE DNA complex. *J. Mol. Biol.*, **314**, 495–506.
79. Qiu,P. and Li,L. (2002) Histone acetylation and recruitment of serum responsive factor and CREB-binding protein onto SM22 promoter during SM22 gene expression. *Circ. Res.*, **90**, 858–865.
80. Pellegrini,L., Tan,S. and Richmond,T.J. (1995) Structure of serum response factor core bound to DNA. *Nature*, **376**, 490–498.
81. Montaner,S., Perona,R., Saniger,L. and Lacal,J.C. (1999) Activation of serum response factor by RhoA is mediated by the nuclear factor-kappaB and C/EBP transcription factors. *J. Biol. Chem.*, **274**, 8506–8515.
82. Hill,C.S., Wynne,J. and Treisman,R. (1995) The Rho family GTPases RhoA, Rac1, and CDC42Hs regulate transcriptional activation by SRF. *Cell*, **81**, 1159–1170.
83. Sotiropoulos,A., Gineitis,D., Copeland,J. and Treisman,R. (1999) Signal-regulated activation of serum response factor is mediated by changes in actin dynamics. *Cell*, **98**, 159–169.
84. Gineitis,D. and Treisman,R. (2001) Differential usage of signal transduction pathways defines two types of serum response factor target gene. *J. Biol. Chem.*, **276**, 24531–24539.
85. Wadman,I.A., Osada,H., Grutz,G.G., Agulnick,A.D., Westphal,H., Forster,A. and Rabbitts,T.H. (1997) The LIM-only protein Lmo2 is a bridging molecule assembling an erythroid, DNA-binding complex which includes the TAL1, E47, GATA-1 and Ldb1/NLI proteins. *EMBO J.*, **16**, 3145–3157.